Remote Sensing of Environment 223 (2019) 95–114

Contents lists available at ScienceDirect

Remote Sensing of Environment

journal homepage: www.elsevier.com/locate/rse

What is global photosynthesis? History, uncertainties and opportunities

Youngryel Ryu[a,*], Joseph A. Berry[b], Dennis D. Baldocchi[c]

[a] Department of Landscape Architecture and Rural Systems Engineering, Seoul National University, South Korea
[b] Department of Global Ecology, Carnegie Institution for Science, Stanford, CA, USA
[c] Department of Environmental Science, Policy and Management, UC Berkeley, Berkeley, CA, USA

ARTICLE INFO

Keywords:
Photosynthesis
Gross primary productivity
Remote sensing
Carbon cycle
Sun-induced chlorophyll fluorescence

ABSTRACT

Quantifying global terrestrial photosynthesis is essential to understanding the global carbon cycle and the climate system. Remote sensing has played a pivotal role in advancing our understanding of photosynthesis from leaf to global scale; however, substantial uncertainties still exist. In this review, we provide a historical overview of theory, modeling, and observations of photosynthesis across space and time for decadal intervals beginning in the 1950s. Then we identify the key uncertainties in global photosynthesis estimates, including evaluating light intercepted by canopies, biophysical forcings, the structure of light use efficiency models and their parameters, like photosynthetic capacity, and relationships between sun-induced chlorophyll fluorescence and canopy photosynthesis. Finally, we review new opportunities with big data and recently launched or planned satellite missions.

1. Introduction

Fifty years ago when the journal *Remote Sensing of Environment* was launched, a landmark workshop on photosynthesis and production was held in Trebon, Czechoslovakia (de Wit, 1970). Held during the Cold War, it was one of the last meetings that combined scientists from the Eastern Bloc, Western Bloc, USA, Australia and Asia until the collapse of the Iron Curtain in 1989. At the meeting, C.T. de Wit argued: "*Seven-stage simulation models by means of which eco-systems may be explained on basis of the molecular sciences are impossible large and detailed and it is naive to pursue their construction.*" He was skeptical about large-scale photosynthesis research as garbage-in, garbage-out. Many heeded his words and were reluctant to upscale research beyond a field crop or forest. However, as we have since learned, there is much need to assess global photosynthesis. Today, new measurement systems enable us to do so regularly with a degree of confidence. Here we evaluate progress in assessing photosynthesis of ecosystems and the globe and ask and answer the question: How much have we advanced global photosynthesis research since then?

Understanding, quantifying and modeling global photosynthesis is crucial for society. Photosynthesis supports production of food, fiber, wood, grain fed to livestock, and fuel for humanity. Global photosynthesis sets the limit of the planetary boundary of production, which has been used widely to quantify how much humans have appropriated global production (Imhoff et al., 2004; Vitousek et al., 1986). Running (2012) proposed net primary productivity (NPP) as a measurable planetary boundary (Rockstrom et al., 2009) and argued that only an additional 5 PgC y^{-1} is available for humanity, which requires a precise estimate of global photosynthesis. Photosynthesis is the essential driver of the global carbon cycle, strongly coupled with the climate system via numerous feedback processes (Heimann and Reichstein, 2008; Sellers et al., 2018), which are related to extreme climate events such as heat waves, drought and flooding (Seneviratne et al., 2014; Zscheischler et al., 2013). Larger year-to-year variations of global land carbon sinks compared to the ocean inferred from atmospheric CO_2 inversions (Gurney et al., 2008) suggest that global land photosynthesis must be quantified accurately. Crop yields and wood production, which must increase with population and economic growth, depend on photosynthesis (Wolf et al., 2015). Hence, if we do not have an accurate estimate for the input of carbon into the carbon cycle, how can we be confident in determining how it is consumed by autotrophs and heterotrophs?

Quantifying global photosynthesis requires meeting multiple grand challenges. It requires understanding the coupled and non-linear biophysical processes that span 14 orders of magnitude in space and time (Jarvis, 1995; Osmond et al., 1980). Over the past several decades, strong collaborations among biochemistry, plant physiological ecology and remote sensing communities have advanced our multiscale understanding of photosynthesis (Beer et al., 2010; Farquhar et al., 1980; Sellers et al., 1997). Substantial uncertainties still remain regarding

* Corresponding author at: Department of Landscape Architecture and Rural Systems Engineering, Seoul National University, Seoul 151-921, South Korea.
E-mail address: yryu@snu.ac.kr (Y. Ryu).

https://doi.org/10.1016/j.rse.2019.01.016
Received 30 November 2018; Received in revised form 8 January 2019; Accepted 12 January 2019
Available online 19 January 2019
0034-4257/

spatial and temporal patterns of photosynthesis. These arise in part from the chosen model algorithms and the model parameters (Medlyn et al., 2005) and from large discrepancies among multiple remote sensing products and land surface models (Anav et al., 2015).

Studies of photosynthesis at the leaf scale have a long and rich history (Field and Mooney, 1986; Laisk and Oja, 1974; Schulze et al., 1994), whereas canopy photosynthesis was measured less before the 1990s. The emergence of networks of eddy covariance flux towers has significantly advanced our understanding of canopy photosynthesis processes (Baldocchi, 2014; Wofsy et al., 1993). However, it is notable that eddy covariance systems directly measure net ecosystem exchange, which has been used to *compute* canopy photosynthesis (Reichstein et al., 2005). Furthermore, flux towers do not represent global scales well, particularly in tropical regions, which are assumed to have high photosynthesis, but for which few data exist (Schimel et al., 2015). Upscaling canopy photosynthesis to the global scale requires gridded forcing datasets of vegetation from remote sensing (Baret et al., 2007; Sellers et al., 1996a; Tucker et al., 2005) and meteorology from reconstructed climate or weather datasets. Substantial uncertainties in vegetation indices remain, which could change trend signs (Zhang et al., 2017a).

Advances in satellite remote sensing have played direct and indirect roles in global photosynthesis research. This research field has a relatively short history, given that humanity's first view of the Earth from space came with Sputnik 1 in 1957 (Tatem et al., 2008). Over the last 60 years, a series of satellite missions opened new opportunities to quantify atmospheric radiative transfer processes (Kaufman et al., 1997; Pinker and Laszlo, 1992), vegetation structure and functions (Myneni et al., 2002; Tucker et al., 1986), and land cover types (Hansen et al., 2013; Townshend et al., 1991), all of which provide key constraints on estimates of global photosynthesis. Previous review papers of remote sensing of photosynthesis have focused on specific tools such as light use efficiency (LUE) (Hilker et al., 2008) and sun-induced chlorophyll fluorescence (Porcar-Castell et al., 2014), or made intercomparisons of global photosynthesis maps from state-of-the-art land surface models and bench-mark datasets (Anav et al., 2015). However, to our knowledge, a comprehensive and contemporary historical review of remote sensing of global photosynthesis including different approaches, from leaf to canopy to continental scale, does not exist.

In this review, we first cover historical achievements in photosynthesis research at a decadal interval from leaf, canopy to the global land (Fig. 1), as this information needs to be coupled to produce accurate bottom up estimates of global photosynthesis. We review key studies in theory, modeling and observations of photosynthesis across scales, which in the end converge to the remote sensing of global terrestrial photosynthesis. Then we identify key uncertainties in global terrestrial photosynthesis research, and discuss new opportunities presented by the emergence of novel remote sensing data sets.

2. Historical overview

2.1. Pre-1970s: few data exist, but theory and modeling are mature

Important theories in photosynthesis were established during this period. At the biochemical level, C3 (Calvin and Benson, 1948) and C4 photosynthetic pathways (Hatch and Slack, 1966; Kortschak et al., 1965) were discovered. To understand photosynthesis at the canopy level, it is crucial to quantify canopy architecture and light environments. Two important achievements were made by a Japanese group, who introduced Beer's Law to quantify light penetration through canopies (Monsi and Saeki, 1953, 2005), and an Estonian group, who pioneered mathematical descriptions for canopy radiative transfer processes (Nilson, 1971; Ross, 1981).

Only a handful of observations of leaf photosynthesis existed, but they provided great insights into photosynthesis processes. At the leaf level, light response curves across diverse species revealed a rectangular hyperbola relationship between light saturation and photosynthesis (Rabinowitch, 1951). Observations of chlorophyll fluorescence of plants under exposure to light after a dark period revealed a sharp increase and gradual decline (Kautsky, 1931), and an inverse relationship to photosynthesis (McAlister and Myers, 1940). Furthermore, relationships between photosynthesis and environmental variables such as oxygen (Björkman, 1966), light (Björkman and Holmgren, 1963), elevation (Billings et al., 1961), CO_2 (Gabrielsen, 1949) and temperature (Schulze et al., 1967) were investigated. Gaastra (1959) comprehensively measured crop photosynthesis against light, temperature, CO_2 and stomata conductance. One key breakthrough was to integrate CO_2 and water vapor in leaf gas exchange measurements, which enabled research on leaf photosynthesis coupled to stomata conductance and transpiration as we see today (Björkman and Holmgren, 1963; Gaastra, 1959; Larcher, 1960).

At the canopy level, chamber systems were widely used to estimate canopy photosynthesis (see review of different types of chamber systems by (Eckardt, 1968)). They were applied to alfalfa and wheat (Thomas and Hill, 1937), pine trees (Tranquillini, 1957), and corn (Moss et al., 1961). Technical issues were carefully tested, including differences in light, temperature, and humidity environments between ambient air and inside chambers (Musgrave and Moss, 1961). Chamber-based carbon gain observations achieved 85 to 99% of actual carbon gain by harvest method in sunflowers and aspen trees (Bate and Canvin, 1971). One important study measured photosynthesis of corn with varying light, temperature, CO_2, and soil moisture conditions and reported remarkable findings: "*Increasing the carbon dioxide concentration increased the assimilation, especially at high light intensities. Small increases in the concentration of carbon dioxide caused large decreases in the stomatal apertures and in transpiration without any decrease in assimilation*" (Moss et al., 1961). This clearly indicated Ribulose 1,5-bisphosphate (RuBP)-limited vs RuBP-saturating rates of photosynthesis and CO_2 fertilization effects on canopy photosynthesis. Another important method for estimating canopy photosynthesis emerged from the field of micrometeorology. An aerodynamic method was applied to wheat (Inoue et al., 1958) and corn (Lemon, 1960) fields. However, daytime CO_2 uptake was attributed to canopy photosynthesis and flux gradient theory was applied, which were both error-prone in canopy photosynthesis estimates. A few groups measured soil respiration to infer canopy photosynthesis from net CO_2 exchange observations (Baumgartner, 1969; Brown and Rosenberg, 1971).

Modeling photosynthesis from leaf to canopy was achieved successfully. At the leaf level, resistance network-based (Gaastra, 1959) and kinetics-based (Laisk, 1970) models were developed. It was essential to quantify leaf temperature to estimate leaf photosynthesis rate correctly, and substantial efforts were made to solve leaf energy balance (Curtis, 1936; Gates, 1968; Raschke, 1960). At the canopy level, a big-leaf model integrating leaf photosynthesis rates with respect to leaf area index was developed and tested (Monsi and Saeki, 1953, 2005). More complete canopy photosynthesis models incorporated leaf angle distributions, separate treatments of beam and scattered radiation penetrating the canopy, separation of sunlit and shaded leaves, and decreasing leaf maximum photosynthetic rates with canopy depth (De Wit, 1959, 1965; Duncan et al., 1967; Monteith, 1965). The Soil-Plant-Atmosphere Model (SPAM) constrained canopy photosynthesis by integrating climate boundary, leaf, soil surface boundary and crop submodels, which were evaluated against comprehensive field observations (Lemon et al., 1971).

Key leaf spectral properties, which later allowed us to link remote sensing to photosynthesis, were first observed in this era. Earlier work focused on spectral reflectance in the visible band with different species and incident angles (Moss and Loomis, 1952; Shull, 1929). Comprehensive surveys were reported for visible to near-infrared (NIR) spectral reflectance across forests, shrubs, mosses, lichens and soils (Krinov, 1953) and far NIR reflectance (3–25 μm) in deciduous trees and herbaceous plants (Gates and Tantraporn, 1952). Comparative analysis

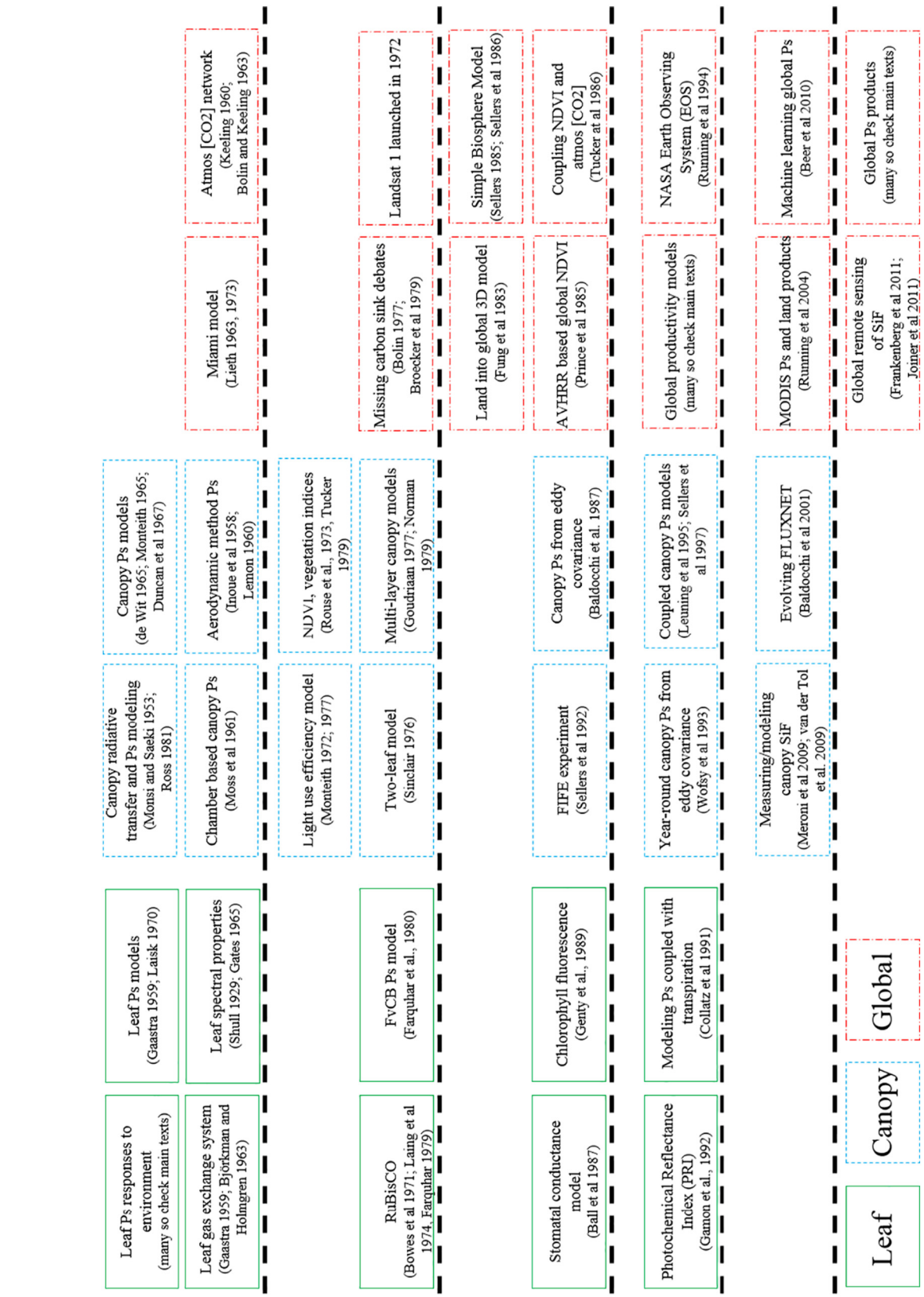

Fig. 1. Summary of historical overview of global photosynthesis studies of Section 2. Ps is photosynthesis.

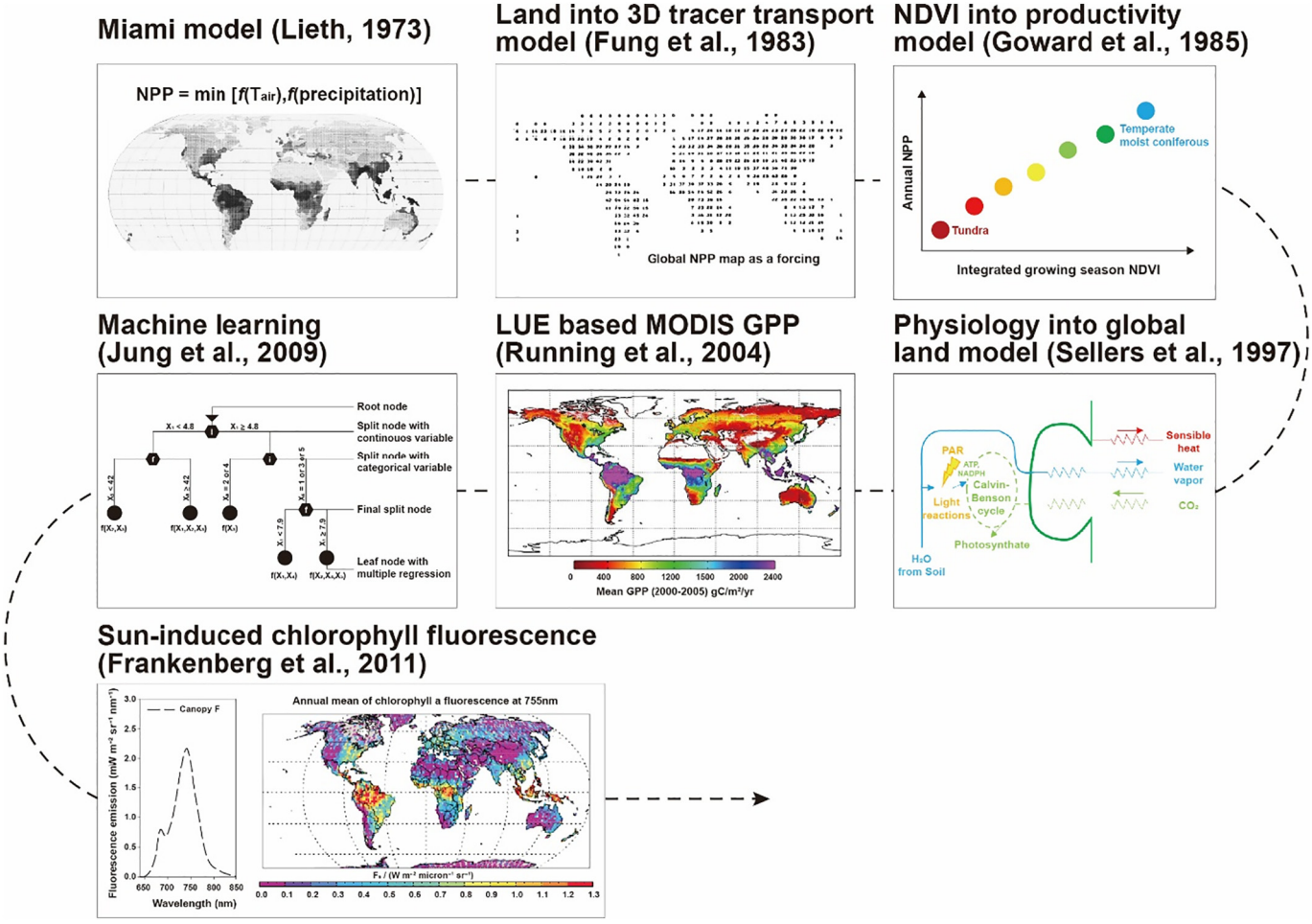

Fig. 2. Milestone works in global photosynthesis estimates. All figures were redrawn or reprocessed.

revealed higher reflectance in both visible and NIR regions in desert species than alpine species (Billings and Morris, 1951). Gates et al. (1965) provided the most comprehensive assessments of the spectral properties of plant leaves and stems across the ultraviolet, visible and NIR regions. The contrast between higher (lower) absorptions in red (NIR) radiation by vegetation motivated one study that monitored leaf area index by measuring the ratio of red to NIR radiation at the forest floor (Jordan, 1969).

Efforts to estimate global NPP emerged, too, with rudimentary computers. The landmark model, the Miami model, applied von Liebig's Law of the minimum to temperature and precipitation, and computed 50 PgC y^{-1} as the global NPP (Lieth, 1963, 1973) (Fig. 2). The Miami model upscaled photosynthesis information with empirical functions forced by coarsely gridded climate variables; it lacked direct information on vegetation. This pioneering estimate of global NPP is within the ball-park of a recent meta-analysis of global NPP (Ito, 2011). It is notable that earlier estimates of global NPP were unrealistically low, such as 24 PgC y^{-1}, based on extrapolating NPP data of the Bavarian forest to the global scale (Ebermayer, 1982), and 13 PgC y^{-1}, based on updating the global land cover map in Ebermayer (1982) (Schroeder, 1919). Application of the Miami algorithms to estimate global photosynthesis by integrating estimates of photosynthesis from FLUXNET, a global network of eddy flux towers (Baldocchi et al., 2001), with gridded climate variables, has produced global estimates of gross primary productivity (GPP) on the order of 150 PgC y^{-1} (Beer et al., 2010). Indeed, the model residual was highly correlated to the annual mean fraction of absorbed photosynthetically active radiation by vegetation (fPAR) (Beer et al., 2010), which confirmed the lack of vegetation information in the Miami model. The Miami model was a reasonable approach at the time, as there was no global map of vegetation properties, which is only possible through satellite remote sensing.

The establishment of long-term atmospheric CO_2 observation networks spanning Mauna Loa, the South Pole, Little America and Point Barrow beginning in the late 1950's must be highlighted. Initial results indicated pronounced seasonal variations of atmospheric CO_2 at Mauna Loa, in contrast to slight seasonal variations with secular increase over the years in Antarctica (Keeling, 1960). Combined with isotopic abundance and seasonal variations of atmospheric CO_2 data, it was concluded that vegetation activity mainly drove the seasonal variations of atmospheric CO_2 observed in the Northern Hemisphere (Bolin and Keeling, 1963; Keeling, 1960). This was one of the first indications of the importance of global photosynthesis, as it inferred the breathing of the biosphere at the global scale.

2.2. 1970s: learning period for remote sensing of global photosynthesis

Discovering biochemical mechanisms of photosynthetic enzymes fundamentally advanced our understanding of leaf photosynthesis. It was reported that ribulose-1,5-bisphosphate carboxylase/oxygenase (RuBisCO) has dual roles of carboxylase and oxygenase (Bowes et al., 1971), and O_2 inhibits photosynthesis via RuBisCO oxygenase (Laing et al., 1974). Laisk and Oja (1974) discovered that leaf photosynthesis at high leaf internal CO_2 partial pressure (Ci) is limited by the regeneration rate of RuBP, which formed the key concept of the A-Ci curve, where leaf photosynthesis is determined by either the RuBP-

saturated rate or RuBP-limited rate. RuBisCO kinetics were successfully modeled (Farquhar, 1979), which became the foundation of the landmark leaf photosynthesis model by Farquhar, von Caemmerer, and Berry (FvCB) (Farquhar et al., 1980). It is notable that a series of leaf photosynthesis models that incorporated the newly discovered processes in different degrees were developed (Hall, 1979; Marshall and Biscoe, 1980; Tenhunen et al., 1976). In the case of C4 photosynthesis, important findings emerged, such as slight variation of quantum yields with O_2, intercellular CO_2 concentration and leaf temperature (Ehleringer and Bjorkman, 1977). Another important variable in photosynthesis modeling is stomatal conductance, as it controls the port through which CO_2 molecules must pass to reach the chloroplasts. An important study constrained potential stomata conductance via environmental stress factors such as temperature and vapor pressure deficit (Jarvis, 1976).

At the canopy scale, three important advances towards modeling photosynthesis were made. The Light Use Efficiency (LUE)-based canopy photosynthesis model, the so-called big-leaf model, was proposed and tested (Monteith, 1972, 1977). The key concept in the big-leaf model was that crop dry matter production is linearly related to the absorbed light, which has been widely used in remote sensing of photosynthesis as dry matter production scales with NPP so photosynthesis, and is suited best for conditions of closed, well-watered canopies with favorable temperature and ample leaf nitrogen. As the light regime and LUE differs between sunlit and shaded leaves in a canopy, the sun/shade two-leaf canopy model was developed (Sinclair et al., 1976). Separation of sunlit and shaded leaves in canopy model is particularly important because of Jensen's inequality (Ruel and Ayres, 1999); the mean of the function is not equal to the function of the mean in nonlinear system such as canopy radiative transfer and photosynthesis models. The multi-layer canopy model appeared as the most sophisticated approach, splitting a canopy into multiple layers with sun/shade separations in each layer (Goudriaan, 1977; Norman, 1979). Aforementioned advancements in enzyme kinetics-based leaf photosynthesis models were not incorporated into these canopy photosynthesis models.

The launch of the Earth Resources Technology Satellite 1 (ERTS-1, later termed, Landsat 1) in 1972 opened a new era in remote sensing of vegetation. It was a near-polar orbiting spacecraft that monitored the entire Earth, equipped with a multispectral scanner (MSS) that included red and NIR bands. Rouse et al. (1973) proposed a band ratio parameter defined as the ratio of the difference in the ERTS radiance values in the NIR and red bands to their sum, which became the famous normalized difference vegetation index (NDVI). They identified a strong correlation between green biomass and transformed vegetation index ($\sqrt{\mathrm{NDVI}+0.5}$) in the Great Plains. Tucker (1979) comprehensively tested different vegetation indices against plant biomass, leaf water content and chlorophyll content, and found that NDVI performed better than the combination of green and red bands. Landsat MSS data was used to track the wheat leaf area index (Wiegand et al., 1979). The emergence of the Landsat programs offered lessons in crop yield monitoring at scales ranging from local to global (Bauer et al., 1986; MacDonald and Hall, 1980).

An important debate over the "missing carbon sink" ignited interest in global carbon cycle research. Historically, the land carbon sink/source was inferred as a residual from the atmospheric, oceanic and anthropogenic carbon emissions budgets. In this era, multiple research groups reported land as a carbon source due to deforestation (Bolin, 1977; Woodwell et al., 1983; Woodwell et al., 1978). The net carbon release from terrestrial ecosystems in 1980 was quantified as 1.8–4.7 $\mathrm{PgC\,y^{-1}}$ (Houghton et al., 1983). On the other hand, Broecker et al. (1979) did not find any compelling evidence for land as a carbon source and concluded that regrowth and enhancement of forest growth roughly canceled out the removal of biomass from deforestation. The debates stemmed from a lack of evidence from datasets such as satellite remote sensing. Indeed, later, comprehensive analysis of Landsat datasets in the tropics revealed that the widely assumed deforestation rate was overestimated (Skole and Tucker, 1993). It must be stressed that global maps of land cover and carbon density were made by merging literature review, field data, and consultations (Olson et al., 1983; Olson et al., 1985). Those maps served as a stepping stone between the Miami model (Lieth, 1973) and remote sensing of global carbon cycles.

2.3. 1980s: integration and scaling-up

This was a unique period during which different disciplines, such as remote sensing, climate modeling, plant physiological ecology, and micrometeorology, were integrated towards quantifying global photosynthesis. In remote sensing, the landmark achievement in this period was to make global maps of NDVI using the Advanced Very High Resolution Radiometer (AVHRR) (Justice et al., 1985). They provided global pictures of vegetation activity, phenology and land cover (Goward et al., 1985; Tucker et al., 1985), which set satellite remote sensing as the key player in global vegetation monitoring. A key finding was that growing season integrated NDVI showed linear relationships to photosynthesis and NPP across diverse ecosystems (Goward et al., 1985; Running and Nemani, 1988). At the same time, the climate modeling community recognized the importance of land in global carbon cycles, which led to the incorporation of land into a three-dimensional tracer transport model (Fung et al., 1983) (Fig. 2). Integration of AVHRR NDVI and atmospheric CO_2 data and modeling led to the conclusion that "*satellite data can be used to estimate terrestrial photosynthesis*" (Tucker et al., 1986).

Dr. Piers Sellers emerged as an integrator of multiple disciplines towards global land surface flux studies, and leader of multi-scaled field studies to test these models at large scales. He combined canopy radiative transfer modeling and satellite remote sensing to make connections between spectral reflectance, photosynthesis and transpiration (Sellers, 1985; Sellers, 1987). He developed a Simple Biosphere Model (SiB), which was incorporated into general circulation models (GCM) to represent land-atmosphere exchanges of CO_2, water vapor and energy fluxes (Sellers et al., 1986). To evaluate satellite- and model-based land surface flux estimates and to develop mechanistic links between remote sensing and land surface fluxes, he initiated important field campaigns such as the First ISLSCP Field Experiment (FIFE), conducted in a prairie in Kansas from 1987 to 1989 (Sellers et al., 1992), and later the Boreal Ecosystem-Atmosphere Study (BOREAS) (Sellers et al., 1995).

Integration of plant physiological ecology and micrometeorology deserves recognition. Previous studies of micrometeorological flux observations focused on short vegetation or bare soils. An important meeting, the International Union of Forest Research Organizations (IUFRO), was held in Knoxville, TN, USA in 1985. It attracted both communities, which introduced the applications of eddy covariance systems into forest ecological research. Of the meeting, Dr. Richard Waring recalled "*Paul Jarvis and I probably commented more than we should have, trying to get the physiologists to make better links to atmospheric science*" (personal communication). The discovery of failures in flux gradient theory within forest canopy layers (Denmead and Bradley, 1985; Legg, 1985) and technological advancements in PC and data storage systems for raw data, fast response infrared gas analyzers with solid state sensors, and 3D sonic anemometers prepared eddy covariance systems for forest carbon cycle studies. The first observation of forest canopy photosynthesis was reported as the difference of net CO_2 fluxes measured above and below forest canopy layers (Baldocchi et al., 1987).

Strong demand for scaling up models of photosynthesis from leaf scale to the global scale emerged. At the global scale, it was already well recognized that the biosphere plays important roles in feedback processes in the climate system (Shukla and Mintz, 1982) and global carbon budgets (Houghton et al., 1983). At the same time, the top-down approach constrained by atmospheric CO_2 data revealed latitudinal distributions in sinks and sources of CO_2, which were mainly driven by the biosphere (Enting and Mansbridge, 1991). Such macro-scale

understanding of CO_2 required comprehensive assessments from a bottom-up approach. FIFE (Sellers et al., 1992), BOREAS (Sellers et al., 1995) and HAPEX-MOBILHY (André et al., 1986) are exemplary upscaling experiments. It is notable that satellite remote sensing became the key component as a forcing for models and a bridge between field plots and coarse grids of GCMs. For instance, FIFE had two clear objectives that included *upscaling* and *application of satellite remote sensing* (Sellers et al., 1992). Theoretical advancements in upscaling of stomata conductance and biophysical processes deserve recognition, too (Jarvis and McNaughton, 1986; McNaughton and Jarvis, 1991; Raupach and Finnigan, 1988).

Different scales and complexity in photosynthesis modeling appeared. At the leaf level, steady-state photochemical yield of Photosystem II was linked to the difference of maximum to steady-state chlorophyll fluorescence (Genty et al., 1989), which later became the foundation of connecting sun-induced chlorophyll fluorescence (SiF) and canopy photosynthesis (van der Tol et al., 2014). A three-dimensional canopy photosynthesis model, MAESTRO, allowed individual crown-level photosynthesis modeling coupled to radiation regime and transpiration (Medlyn, 2004; Wang and Jarvis, 1990). A semi-empirical stomata conductance model as a function of photosynthesis, relative humidity and atmospheric CO_2 concentration worked well across diverse environmental conditions (Ball et al., 1987). Enzyme kinetics-based C3 and C4 leaf photosynthesis models integrated with the semi-empirical stomata conductance model and transpiration were developed for coupling with GCMs (Collatz et al., 1991; Collatz et al., 1992). In contrast to those bottom-up efforts, top-down global photosynthesis estimates relied on simple LUE approaches. For example, 0.625 $gC\,MJ^{-1}$ of LUE was applied to the global land (Heimann and Keeling, 1989). Accumulated NDVI over the year showed a strong linear relationship to annual NPP across diverse ecosystems, implying a constant LUE (Goward et al., 1985) (Fig. 2).

2.4. 1990s: global photosynthesis and Earth Observing System, EOS

After intensive debates about a “missing carbon sink”, it became evident that global land served as a carbon sink (Ciais et al., 1995; Keeling et al., 1996; Siegenthaler and Sarmiento, 1993; Tans et al., 1990). Ten years of AVHRR NDVI data also supported increased plant growth in the northern high latitude regions (Myneni et al., 1997). Those pieces of evidence only indicated net carbon balance, which must be partitioned among photosynthesis, respiration, and other factors such as fire and land cover change. Interest and urgency related to global photosynthesis research exploded. In this decade, numerous global productivity models were developed, such as DEMETER (Foley, 1994), BIOME (Prentice et al., 1992), BIOME3 (Haxeltine and Prentice, 1996a), TEM (Melillo et al., 1993), CASA (Potter et al., 1993), TURC (Ruimy et al., 1996), CARAIB (Warnant et al., 1994), the Frankfurt Biosphere Model (Lüdeke et al., 1994), a model from University of Sheffield (Woodward et al., 1995), and GLO-PEM (Prince and Goward, 1995). Among them, only a few models, such as CASA, GLO-PEM and TURC, adopted satellite remote sensing to prepare key forcings such as fPAR.

Improvements in LUE models were notable during this decade. First, LUE was not held constant globally anymore (Heimann and Keeling, 1989). Second, LUE was biome-dependent but constant over time (Ruimy et al., 1994). Third, stress factors constrained LUE, which varied in space and time (Potter et al., 1993). A group from the University of Montana used all available satellite remote sensing data, including NDVI, leaf area index (LAI) and land surface temperature, to constrain biome-dependent LUEmax (Nemani and Running, 1989; Running, 1990). A physiologically-based approach for LUE, Physiological (or Photochemical) Reflectance Index (PRI), deserves recognition as well (Gamon et al., 1992). PRI was correlated to epoxidation state of the xanthophyll cycle pigments and Photosystem II quantum yields, which was detectable at 531 nm (Penuelas et al., 1995).

The NASA Earth Observing System (EOS) program set the platform for global photosynthesis research. A brief history includes planning for NASA EOS in 1983, an Announcement of Opportunity to select science investigations for EOS in 1988, the selection of teams in 1989, and the authorization of the NASA EOS program by the US Congress in 1990 (Asrar and Dokken, 1993; Running et al., 1994). In the 1990s, substantial discussions and efforts for implementing the EOS program were made (Justice et al., 1998; Sellers and Schimel, 1993). It was evident that substantial uncertainties in AVHRR NDVI (Goward et al., 1991) and AVHRR land cover maps (Townshend et al., 1991) did not meet the standards in monitoring global vegetation and carbon cycles. The Moderate Resolution Imaging Spectroradiometer (MODIS) onboard Terra and Aqua platforms aimed to achieve better performance than AVHRR in terms of radiometric, spectral, and geometric properties and became the key instrument in the EOS program (Justice et al., 1998; Running et al., 1994). MODIS science teams aimed to develop key land surface process products such as reflectance, albedo, land surface temperature, vegetation indices, land cover, LAI and fPAR, which were all used to compute photosynthesis, the final downstream product (Running et al., 2000). One important aspect of the EOS program was envisioning and supporting field observations for calibration/validation of EOS missions (Baldocchi et al., 1996; Running et al., 1999). It supported establishing flux tower sites across diverse ecosystems, which laid out the foundation of FLUXNET (Baldocchi et al., 2001). In parallel, networks of eddy flux towers at continental scales were initiated in Europe in 1996 (Aubinet et al., 2000; Valentini et al., 2000) and in North America in 1997. During this period, eddy covariance systems enabled year-round monitoring of ecosystem CO_2 flux (Black et al., 1996; Wofsy et al., 1993). Together with expansions in flux tower networks, long-term, ground-based CO_2 flux observations began.

This was a golden era of coupled photosynthesis models, as well. Photosynthesis-transpiration-radiation-wind coupled canopy models were developed and tested (Baldocchi and Meyers, 1998; Chen et al., 1999; Leuning et al., 1995; Sellers et al., 1997). Multiple constraints on photosynthesis modeling via coupling processes provided better mechanisms for controlling spatial and temporal variations in canopy photosynthesis. In particular, coupling of photosynthesis with transpiration via stomata conductance was key to success (Collatz et al., 1991; Leuning, 1995). Incorporation of such a coupled photosynthesis model into GCM avoided the “stomata suicide” problem and advanced canopy photosynthesis modeling at a global scale (Randall et al., 1996; Sellers et al., 1996b) (Fig. 2).

2.5. 2000s: hand-shaking between remote sensing and flux measurements, MODIS and FLUXNET

MODIS instruments were successfully launched aboard Terra and Aqua satellites in 1999 and 2002, respectively, which opened a new era in monitoring global photosynthesis. The MODIS GPP team led by Dr. Steve Running produced eight daily, 1-km spatial resolution GPP products beginning in March 2000 (Running et al., 2004) (Fig. 2). It was based on the LUE approach where LUEmax parameters were biome-dependent, down-regulated with environmental variables such as temperature and vapor pressure deficit. Although most forcing data at the land surface were around 1-km resolution from MODIS Land products, atmospheric forcing data such as solar radiation, temperature and humidity were around 100-km resolution, derived from the NASA Data Assimilation Office (DAO). It turned out that MODIS GPP estimates were highly sensitive to the uncertainties in the DAO data (Zhao et al., 2006).

Substantial efforts were made to evaluate and improve MODIS GPP products against FLUXNET data. Comprehensive upscaling experiments such as the BigFoot project integrated high spatial resolution satellite images such as Landsat with flux tower data and the Biome-BGC model to produce regional scale (5 by 5 km) GPP maps, which were used to evaluate the MODIS GPP product (Turner et al., 2006; Turner et al.,

2003). Uncertainties in MODIS GPP were attributed to underestimation of LUEmax at highly productive sites (Turner et al., 2006), the biases of the MODIS fPAR product in boreal forests during spring (Turner et al., 2003), and uncertainties in atmospheric forcing data (Heinsch et al., 2006). The improved version of the MODIS GPP product showed the global mean GPP between 2001 and 2003 as 109 PgC y^{-1} (Zhao et al., 2005).

With more and more available data in FLUXNET and global land surface remote sensing products from different space agencies, different approaches from the MODIS GPP algorithm emerged to quantify global photosynthesis. First was the machine learning approach. As FLUXNET data covers global climate space well, it appears ready to develop statistical models that are trained and tested against FLUXNET data from continental (Papale and Valentini, 2003; Xiao et al., 2010; Yang et al., 2007) to global scales (Beer et al., 2010; Jung et al., 2009) (Fig. 2). Such machine-learning-based GPP maps became the benchmark for land surface models (Bonan et al., 2011). Second was the choice and availability of a diverse set of vegetation indices. Multiple groups reported that simple vegetation indices such as the Enhanced Vegetation Index (EVI) (Huete et al., 2002) performed better than the MODIS GPP product in tracking seasonal variation of GPP across diverse ecosystems (Huete et al., 2008; Sims et al., 2006). Integrating EVI (Huete et al., 2002) with MODIS Land Surface Temperature product better considered drought effects, which further improved the EVI-based GPP model (Sims et al., 2008). Third was to refine the LUE approach. PRI as an indicator of LUE was widely investigated from leaf to ecosystem scales (see the review (Garbulsky et al., 2011)). In particular, MODIS band 11 centered on 530 nm was used to generate PRI maps (Drolet et al., 2008), and sun-target-sensor geometry was explicitly considered to consider different sensitivity of PRI to leaves in the sun and shade (Hall et al., 2012) and upscale LUE from leaf to landscape (Hilker et al., 2009). Another LUE algorithm that was downregulated with the ratio of latent heat flux to net radiation enabled coupling of carbon and water fluxes at the global scale (Yuan et al., 2010). Fourth was to assimilate FLUXNET, satellite, and leaf traits data into land surface models. Land surface models revealed high uncertainty in predicted phenology (Stockli et al., 2008; Williams et al., 2009). Assimilating the MODIS LAI product into a land surface model improved GPP estimates by 25% compared to the FLUXNET dataset (Demarty et al., 2007). Seasonal variations of photosynthetic capacities in different ecosystems were inferred from FLUXNET datasets, which were incorporated into a land surface model and improved GPP estimates. Extensive leaf trait datasets (Kattge et al., 2011) with FLUXNET data helped to identify deficiencies in the structure of a land surface model, which led to improved GPP estimates (Bonan et al., 2012).

Evolution of SiF research deserves credit. Unlike the other vegetation indices, SiF is linked more directly to photosynthesis as light intercepted by chlorophyll in leaves is used for photochemistry, non-photochemical quenching, and fluorescence (Maxwell and Johnson, 2000). Intensive work in retrieval algorithms (Guanter et al., 2007), field instruments (Moya et al., 2004), and canopy modeling (van der Tol et al., 2009) appeared (see the reviews by (Meroni et al., 2009; Porcar-Castell et al., 2014)). In 2005, the Fluorescence Explorer (FLEX) satellite mission proposal was submitted to the European Space Agency Earth Explorer Program call, which was awarded for funding in 2015, and will be launched in 2022. In this decade, most SiF studies focused on leaf to landscape scales.

2.6. 2010s: machine learning and SiF

We may look back and consider the current decade as the heyday for remote sensing of global photosynthesis. Before this period, only a few groups in the world produced global photosynthesis maps equipped with strong enough computing resources. Owing to the exponential increase in computing power at lower cost (Waldrop, 2016) and emerging platforms such as cloud computing (Agarwal et al., 2011), Google Earth Engine (Gorelick et al., 2017) and NASA Earth Exchange (Nemani et al., 2011), individual scientists were able to handle huge amounts of satellite remote sensing data. Furthermore, standardized and preprocessed remote sensing products in photosynthesis and/or forcing variables used to compute photosynthesis enabled individual scientists to analyze and produce global photosynthesis maps more easily (Jiang and Ryu, 2016; Jung et al., 2017).

Diverse approaches to quantifying global photosynthesis at different complexities appeared. The simplest case was NIRv, which is the product of NDVI and NIR reflectance (Badgley et al., 2017). NIRv isolates vegetation signals from background soils and has potential to be applied to the long-term AVHRR datasets given red and NIR reflectance only. An improved version of the LUE approach integrated EVI to compute fPAR by chlorophyll and land surface water index (Xiao et al., 2002) to constrain LUE, and produced global photosynthesis maps over the MODIS era (Zhang et al., 2017b). A different LUE model that adopted an optimality hypothesis (Haxeltine and Prentice, 1996b) predicted global C3 photosynthesis with APAR, atmospheric CO_2 concentrations, vapor pressure deficit, temperature and elevation (Wang et al., 2017). A simplified process based model coupled photosynthesis with atmospheric radiative transfer (Ryu et al., 2018), canopy radiative transfer, transpiration, stomata conductance and leaf energy balance by merging multiple satellite remote sensing datasets to produce global maps of photosynthesis in C3 and C4 over the MODIS era (Jiang and Ryu, 2016; Ryu et al., 2011).

Machine learning became more popular with better computing power and more data. A machine learning algorithms intercomparison project, FLUXCOM, was initiated and upscaled FLUXNET-based photosynthesis data to continental and global scales (Jung et al., 2017; Tramontana et al., 2016). Recently, machine learning methods produced global photosynthesis, net ecosystem exchange, and energy flux maps at half-hourly intervals between 2001 and 2014 (Bodesheim et al., 2018). Incorporating SiF into a machine learning algorithm reduced uncertainties in global photosynthesis maps (Alemohammad et al., 2017). The success of the machine learning approach depends on the representativeness of FLUXNET datasets in terms of spatial (Papale et al., 2015) and temporal (Chu et al., 2017) domains, and data for the tropics are still lacking (Schimel et al., 2015).

Intensive work on SiF during this period deserves recognition. The first global maps of SiF from the Japanese satellite GOSAT were tightly correlated with the machine learning-based global photosynthesis maps (Frankenberg et al., 2011; Joiner et al., 2011) (Fig. 2). A series of papers reported the superior performance of SiF over conventional vegetation indices for tracking seasonal variations of photosynthesis across diverse ecosystems (Guanter et al., 2014; Joiner et al., 2014; Sun et al., 2017) and for identifying earlier response of canopy stresses (Rascher et al., 2015; Rossini et al., 2015). The Global Ozone Monitoring Experiment-2 (GOME-2)-based SiF product has been widely used, but it offers an infrequent, spatially coarse dataset (biweekly, 0.5°) (Joiner et al., 2013). One recent study used a machine learning approach to reproduce GOME-2 SiF at finer spatial and temporal resolutions corresponding to MODIS (Gentine and Alemohammad, 2018). The TROPOspheric Monitoring Instrument (TROPOMI) launched in 2017 appears to be a game changer; it is used to produce global maps of SiF at resolutions up to 7 by 3.5 km with daily revisit frequency globally (Köhler et al., 2018).

3. Uncertainties

In spite of substantial advances in theory, observation and modeling of photosynthesis over more than five decades, global photosynthesis estimates are still highly uncertain (Fig. 3). One recent review of global photosynthesis estimates from diverse remote sensing products and land surface models reported that annual sum values ranged from 112 to 169 PgC y^{-1}, interannual variability ranged from 0.8 to 4.4 PgC y^{-1}, and trends varied from 0.005 to 0.621 PgC y^{-2} (Anav et al., 2015). In a

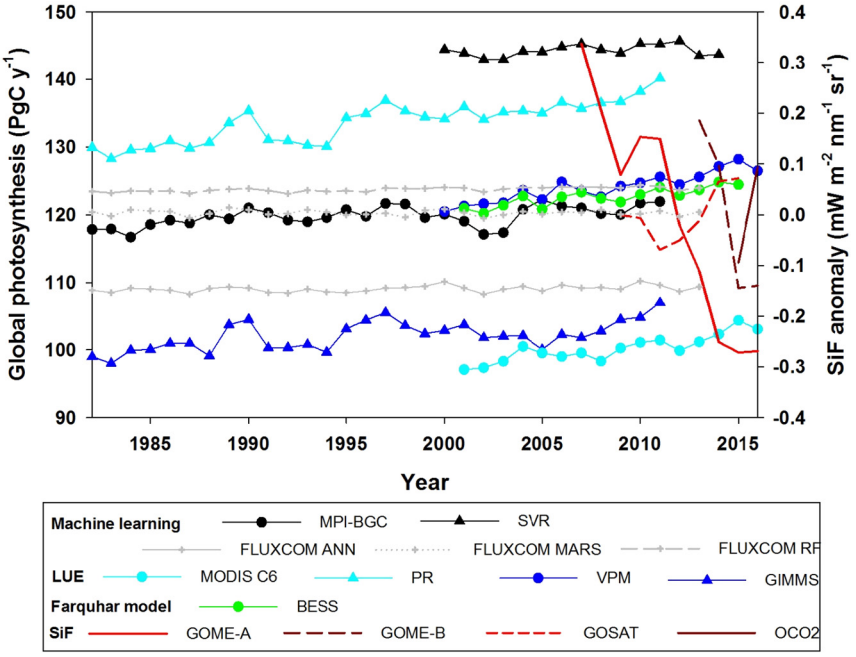

Fig. 3. Time series of annual global photosynthesis and SiF estimates from different remote sensing based products. SiF datasets present annual anomaly values adopted from (Luo et al., 2018). Data sources include: MPI-BGC (Jung et al., 2010), SVR (Kondo et al., 2015), FLUXCOM (Jung et al., 2017), MODIS C6 GPP product (Running et al., 2004), PR (Keenan et al., 2016), VPM (Zhang et al., 2017b), GIMMS (Smith et al., 2016), BESS (Jiang and Ryu, 2016), GOME (Joiner et al., 2013), GOSAT (Frankenberg et al., 2011), and OCO2 (Sun et al., 2017).

synthesis of work on the North American Carbon Program that involved 26 models and data from 39 flux tower sites, none of the models were able to predict GPP estimates within the observed uncertainty (Schaefer et al., 2012).

We review the main sources of uncertainty in the framework of LUE. The key steps in quantifying global photosynthesis estimates include incoming PAR and diffuse fraction of PAR, intercepted PAR by canopy (APAR) which is determined by canopy structure, and LUE which represents how much APAR is converted to canopy photosynthesis. One example appears in Fig. 4 that was simulated from Breathing Earth System Simulator (BESS) that couples atmospheric and canopy radiative transfer, transpiration, stomata conductance, leaf energy balance and photosynthesis using multiple satellite remote sensing datasets (Jiang and Ryu, 2016; Ryu et al., 2011). Maximum LUE on an annual scale appears 2%, consistent with FLUXNET synthesis (Baldocchi and Penuelas, 2019), but how much actual LUE deviates from the maximum LUE is under high uncertainty. It is notable that maximum LUE appears in the wet tropics characterized by favorable temperature, ample water, long growing season, and high ratio of diffuse light.

3.1. Light intercepted by canopies

3.1.1. Solar radiation

The fundamental driver of canopy photosynthesis is solar radiation, but surprisingly, globally gridded solar radiation maps involve substantial uncertainties. One study that compared four remote sensing-based global solar radiation products reported consistent overestimation of magnitudes, but with different trends and interannual variability (Zhang et al., 2015b). The high uncertainties in global solar radiation datasets led Jung et al. (2011) to not use solar radiation as an explanatory variable in their machine learning-based global photosynthesis product. Multiple long-term, global solar radiation datasets exist, but global PAR datasets are rare. Therefore, using a constant ratio to convert solar radiation into PAR was a common approach applied in widely used products such as the MODIS GPP product (Running et al., 2004). It is, however, well known that the ratio of PAR to solar radiation varies with altitude, water vapor content and view zenith angle; on an annual mean scale, the ratio varies from 0.41 to 0.53 across the global land surface (Ryu et al., 2018). Furthermore, the diffuse fraction of PAR is important for canopy photosynthesis modeling as diffuse radiation can penetrate deeper into canopies and thus enhance LUE (Knohl and Baldocchi, 2008; Mercado et al., 2009); however, global maps of diffuse PAR are lacking. It is notable that most global photosynthesis products have relied on coarse solar radiation datasets (0.5 to 1° resolution) while using fine-resolution (around 1 km) land surface property datasets, which led to a substantial scale mismatch between atmosphere and land surface forcings (Running et al., 2004; Yuan et al., 2010; Zhang et al., 2017b). Recently, MODIS-based solar radiation, PAR and diffuse PAR products were developed at a daily, 5 km resolution since 2000 (Ryu et al., 2018) (Fig. 4). An official MODIS land surface radiation product that includes solar radiation and total PAR now provides beta version datasets at a daily, 5 km resolution (Wang, 2017). Development of accurate, high spatial and temporal resolution radiation maps going back to 1982 are urgently needed to reduce uncertainties in trends of global photosynthesis estimates.

3.1.2. Canopy structure

Canopy structure determines how much incoming solar radiation the canopy intercepts.

$$i_0 = 1 - \exp\left[-\frac{\mathrm{LA}\Omega(\theta)\mathrm{G}(\theta)}{\cos(\theta)}\right] \quad (1)$$

where i_0 is the canopy interception of directional light, Ω is the clumping index, G is the leaf projection function, and θ is the view zenith angle. Therefore, LAI, leaf angle distribution and clumping index must be quantified to compute the fraction of light intercepted by the canopy. Theories of canopy radiative transfer processes are mature (Myneni et al., 1989; Ross, 1981; Stenberg et al., 2016); however, preparation of accurate forcing data and key parameters appears to be challenging. For example, a recent comprehensive study that compared four long-term satellite LAI products between 1982 and 2011 revealed that they were inconsistent in terms of magnitudes, interannual variations and trends across products, and were not self-consistent over time, particularly owing to AVHRR orbit changes (Jiang et al., 2017). The MODIS product was affected by sensor degradation. Updates of the MODIS land surface reflectance product from Collection 5 to 6 changed the global vegetation trends from browning to greening (Zhang et al., 2017a). The GLOBMAP LAI product that combined MODIS Collection 5 and AVHRR datasets (Liu et al., 2012) showed a pronounced declining trend after 2000 (Jiang et al., 2017), which was reversed after using the

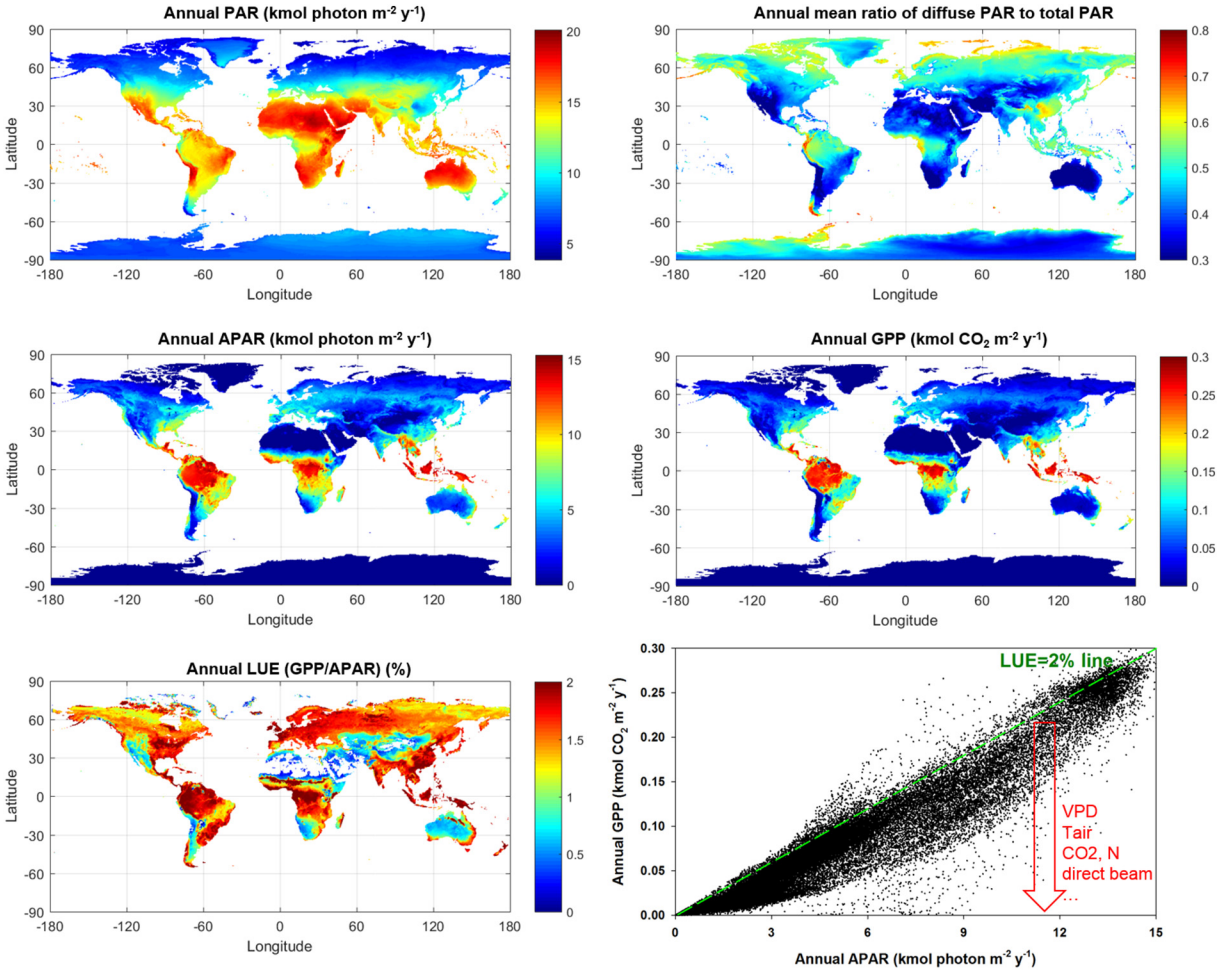

Fig. 4. Global maps of photosynthetically active radiation (PAR), ratio of diffuse to total PAR, absorbed PAR by canopy (APAR), gross primary productivity (GPP), and light use efficiency (LUE, the ratio of GPP to APAR) between 2001 and 2016 simulated by Breathing Earth System Simulator (BESS) forced with multiple sources of satellite remote sensing datasets (Jiang and Ryu, 2016; Ryu et al., 2011). All data are mean annual sum values over the 16 years. The scatterplot between APAR and GPP indicates that maximum LUE is around 2%, and actual LUE departs from the maximum LUE with biotic and abiotic factors, which is the key to estimate GPP correctly.

MODIS Collection 6 dataset. A study that compared three global LAI products reported relative uncertainty greater than 20%, with higher uncertainties in forest regions (Fang et al., 2012). To compute LAI from canopy radiative transfer models, a spherical leaf angle distribution (Nichiporovich, 1961) or biome-dependent leaf angle distributions commonly have been assumed (Knyazikhin et al., 1998). However, field observations on diverse tree species in temperate to boreal forests have revealed that the majority of species had planophile or plagiophile leaf angle distributions (Pisek et al., 2013). Terrestrial LiDAR (Bailey and Mahaffee, 2017) and digital leveled photography (Ryu et al., 2010) offer novel methods to quantify leaf angles easily, and it is time to move beyond spherical leaf angle distribution through more in-situ data and better parameterization. The clumping index is angle-dependent and its behavior is complex. For example, the clumping index increased with view zenith angle in boreal forests (Kucharik et al., 1999), while it decreased with view zenith angle in a savanna ecosystem (Ryu et al., 2010). Such contrasting behavior is related to the scales of clumping from shoots, within and between tree crowns, which presents a challenge in remote sensing of clumping index. Multi-angular, remote sensing-based global clumping index maps are available (Chen et al., 2005; Wei and Fang, 2016), however, incorporating all scales of clumping effects requires substantial further efforts.

3.2. Light use efficiency

Since LUE was proposed as a concept in a seminal paper by Monteith (1977), numerous approaches have been developed to down-regulate LUE with environmental stress factors.

$$\text{LUE} \sim f(\text{air temperature, vapor pressure deficit, soil moisture, C3 or C4, fraction of diffuse light, } CO_2, \text{N}) \quad (2)$$

3.2.1. Forcing data

The most direct uncertainty in the LUE approach is caused by uncertainty in the forcing data. Air temperature and vapor pressure deficit data are available over land globally from data assimilation systems, which combine satellite remote sensing and weather station data, such as MERRA (Rienecker et al., 2011), ERA (Uppala et al., 2005) and NCEP (Kalnay et al., 1996). One study used three global weather datasets to test the sensitivity of global photosynthesis estimates from the LUE algorithm of the MODIS GPP product. It reported that the choice of weather dataset can change global photosynthesis estimates by more than 20 PgC y^{-1} (Zhao et al., 2006). Satellite microwave remote sensing offers a global picture of soil moisture, but it only covers a few cm depth in the top soil layer (Entekhabi et al., 2010; Kerr et al., 2010). Such shallow soil moisture information is still useful to understand global water cycles (McColl et al., 2017); however, root zone soil

moisture status, which is directly related to canopy photosynthesis, is unlikely to be captured. Other proximal indices related to soil moisture are available, such as normalized difference water index (Gao, 1996) and land surface water index (Xiao et al., 2002), which both use NIR and shortwave infrared channels. However, separating soil moisture information from vegetation water status is elusive.

Global maps of C4 distribution are important as C4 species account for ~25% of global photosynthesis and C4 photosynthetic processes differ fundamentally from those of C3 species (Still et al., 2003). It is notable that machine learning-based global photosynthesis maps such as FLUXCOM and MPI-BGC (Beer et al., 2010; Jung et al., 2017) did not consider C4 photosynthesis explicitly, likely resulting in underestimating global photosynthesis. The most widely used C4 distribution dataset offers a 1° spatial resolution, static map of C4 fraction in vegetation by merging climate rules, crop fraction maps, and vegetation continuous fields maps (Still et al., 2003), which were recently updated to 0.5° resolution (Wei et al., 2014). However, those C4 maps still contain substantial uncertainties. For example, in savanna ecosystems, trees are C3 while a dynamic fraction of grasses are C4 (Whitley et al., 2017), which is very difficult to quantify. Also, static C4 fraction maps are unable to capture rotations of C3 and C4 crops. Global land cover maps are still uncertain. Important parameters to retrieve canopy structure (Knyazikhin et al., 1998) and canopy physiology (Kattge et al., 2009) are dependent on land cover types. Spurious interannual variability of land cover types could lead incorrect interannual variations of canopy photosynthesis (Jiang and Ryu, 2016). Substantial advancements in global land cover mapping have been achieved (Friedl et al., 2010; Gong et al., 2013), but further improvements that capture agricultural expansion, urbanization, tropical deforestation, temperate reforestation/afforestation precisely at global scale are required to estimate global photosynthesis variations better. Advanced global land cover maps will improve global maps of leaf traits (Moreno-Martínez et al., 2018).

3.2.2. LUE model structure

The MODIS GPP product algorithm down-regulates LUE with low air temperature and high vapor pressure deficit (Running et al., 2000), which forces the model to increase (decrease) LUE in colder (warmer) regions with global warming. Based on MODIS GPP/NPP products, one paper reported a decrease of global NPP due to droughts, particularly in the Southern Hemisphere between 2000 and 2009 (Zhao and Running, 2010), which was criticized as the LUE model structure in MODIS GPP algorithm forced to decrease GPP in warmer Southern Hemisphere (Medlyn, 2011). A recent study investigated the reduction of LUE due to soil moisture separated from vapor pressure deficit and MODIS EVI using FLUXNET datasets, and reported that soil moisture alone could reduce annual photosynthesis estimates by up to 40% (Stocker et al., 2018). This indicates that down-regulation of LUE with vapor pressure deficit is not able to capture drought effects well. However, as discussed above, it is questionable whether we have a global soil moisture dataset of sufficiently high quality to accurately constrain LUE. A synthesis paper using a FLUXNET dataset also reported that seasonal variations of LUE are more strongly related to the water availability (ratio of *actual* evaporation to potential evaporation) or energy balance (the ratio of *actual* evaporation to net radiation) than to the vapor pressure deficit (Garbulsky et al., 2010). However, remote sensing of *actual* evaporation under drought conditions remains a challenge (Yang et al., 2015b).

In the coordination hypothesis, the FvCB photosynthesis model was incorporated into an LUE framework by assuming that actual photosynthesis rate appears when RuBisCO-limited and electron transport-limited photosynthetic rates are equal (Wang et al., 2017). This assumption allows us to compute the ratio of intercellular to ambient CO_2 concentrations and thus to consider CO_2 fertilization effects (Keenan et al., 2016), which were ignored in previous LUE frameworks. This hypothesis is attractive as multiple satellite remote sensing platforms monitor atmospheric CO_2 concentrations globally (Kuze et al., 2009; Schwandner et al., 2017). However, it requires further evidence; the modeled ratio of intercellular to ambient CO_2 concentrations only explained 25% of the variations of the field observations (Wang et al., 2017).

PRI has been used widely as a proxy for LUE (Eq. (2)). Although PRI performed well in tracking LUE from leaf to canopy to ecosystem scale (Garbulsky et al., 2011), several key challenges remain to applying PRI to estimate global photosynthesis. First, PRI was originally developed to detect spectral changes related to the xanthophyll cycle and LUE at the diurnal time scale (Gamon et al., 1992). On seasonal scales, leaf carotenoid and chlorophyll pigment pools or their ratio, rather than the xanthophyll cycle, drive PRI variations (Filella et al., 2009; Gamon et al., 2016; Hmimina et al., 2015). Therefore, a recent study proposed the chlorophyll/carotenoid index (CCI) by combining MODIS bands 11 (centered on 530 nm) and 1 (centered on 645 nm), which tracked seasonal variations of canopy photosynthesis in evergreen canopies (Gamon et al., 2016). It is notable that the CCI tracked seasonal variations of photosynthesis, not LUE. Applying PRI to estimate LUE across a range of temporal scales requires careful attention. Second, global maps of surface reflectance at 531 nm with atmospheric correction are not available, which forced a few individual researchers to process MODIS band 11 for specific sites or regions (Drolet et al., 2008; Gamon et al., 2016). Third, it is unclear whether PRI could capture LUE variations in tropical forests. One study conducted continuous observations of PRI and LUE in an evergreen broadleaf forest in Malaysia over three years, and reported that PRI only explained 12% of variations in LUE (Nakaji et al., 2014). In the study, VPD alone explained 34% of variations in LUE, and the combination of PRI and VPD into a multiple regression model showed the best performance, explaining 38% of LUE variations. In a sub-tropical coniferous forest, PRI explained 20% and 29% of variations in LUE at half-hourly and daily intervals, respectively, and showed little correlation with LUE during favorable weather conditions (Zhang et al., 2015a). Fourth, there was a lack of a process-based model to simulate the spectral changes related to the xanthophyll cycle that are used in the PRI (Coops et al., 2010). It is noteworthy that very recently, the xanthophyll cycle was incorporated into the SCOPE model, which permits simulation of PRI behavior over time and space (Vilfan et al., 2018). We expect this will further advance our understanding of the information present in PRI as well as providing the tools to investigate the potential to use more than two wavelengths in the spectral region 500–570 nm to maximize the information relevant for photosynthesis estimation.

3.2.3. Cloudy conditions

Our inability to monitor LUE from space under cloudy conditions poses a challenge in global photosynthesis estimates. In particular, clouds are pervasive in the tropical and temperate regions that account for more than 70% of global annual photosynthesis (Beer et al., 2010). It is well known that diffuse light can penetrate deeper into the canopy, which enhances photosynthesis in shaded leaves, thus increasing canopy-level LUE (Knohl and Baldocchi, 2008; Niyogi et al., 2004; Roderick et al., 2001). However, optical satellite remote sensing provides information about the canopy structure and function only under cloud-free conditions; cloudy data are gap-filled using non-cloudy data (Zhao et al., 2005), which is likely to underestimate canopy level LUE. In a conventional multiplicative form of the LUE model (Eq. (2)), enhancement of LUE under cloudy conditions has largely been ignored (Running et al., 2004; Yuan et al., 2010). PRI increases with shadow fraction (Drolet et al., 2008; Hilker et al., 2009); therefore, missing satellite PRI information on cloudy days would lead to underestimation of PRI. Often, land surface temperature from thermal remote sensing has been used to constrain LUE (Sims et al., 2008), but land surface temperature data also is not available under cloudy conditions.

3.2.4. Photosynthetic capacity

Leaf nitrogen contents are tightly correlated to maximum

carboxylation rate (Field and Mooney, 1986; Kattge et al., 2009), which is a key parameter in the FvCB photosynthesis model. More recently, it was shown that phosphorus content can modify this relationship (Walker et al., 2014). As the majority of global ecosystems are nitrogen-limited, it is essential to quantify spatial and temporal patterns of leaf nitrogen at global scales to improve global photosynthesis estimates. One study reported that canopy nitrogen contents scale with NIR reflectance in temperate to boreal forests (Ollinger et al., 2008). However, another group argued that the good correlation between canopy nitrogen contents and NIR reflectance was an artifact caused by variations in canopy structure across sites (Knyazikhin et al., 2013b), which led to further debates (Knyazikhin et al., 2013a; Townsend et al., 2013). In fact, it is well known that the most direct absorption signal related to protein and nitrogen content is located in the short-wave infrared part of the spectrum (Curran, 1989; Kokaly, 2001). However, this signal is not only weak, but also partly masked by the much stronger water absorptions, which makes it hard to retrieve using process-based methods such as radiative transfer model inversion (Jacquemoud et al., 1996). Nevertheless, some advances in model inversion-based leaf nitrogen content estimates have emerged, even at the canopy level (Wang et al., 2018), which require further evaluation. Statistical methods have been applied successfully to quantify leaf nitrogen contents both at the leaf (Asner et al., 2011; Dechant et al., 2017) and canopy scales (Asner et al., 2015; Singh et al., 2015); however, as for the radiative transfer model inversion, hyperspectral data that is currently unavailable is required. With growing leaf trait databases, maximum carboxylation rate has become better constrained for plant functional types (Ali et al., 2015; Kattge et al., 2009) and global static maps of nitrogen-based maximum carboxylation rates are available (Walker et al., 2017). However, a growing body of literature suggests that maximum carboxylation rates show large seasonal variations (Muraoka and Koizumi, 2005; Wilson et al., 2000; Xu and Baldocchi, 2004; Yang et al., 2018b), which was incorporated into a land surface model via model-data fusion framework (Wang et al., 2007).

Several authors have argued that leaf chlorophyll contents can be used as a proxy for maximum carboxylation rates (Alton, 2017; Croft et al., 2017; Houborg et al., 2013). One study proposed connections between chlorophyll contents, leaf nitrogen contents, RuBisCO enzyme kinetics, and maximum carboxylation rates, which were tested in a corn field site (Houborg et al., 2013). A recent field study on four deciduous species reported that chlorophyll contents, rather than leaf nitrogen contents, were better correlated to maximum carboxylation rates (Croft et al., 2017). Linking chlorophyll contents with photosynthetic capacity seems partly motivated by a more straightforward estimation of chlorophyll content from remote sensing observations compared to nitrogen content. However, contrary to a large volume of leaf trait data that supported relationships between leaf nitrogen contents and photosynthetic capacity (Kattge et al., 2009), few chlorophyll content and photosynthetic capacity data exist. Furthermore, a mechanistic understanding of their relationship appears incomplete. Recently, global monthly maps of photosynthetic capacity at 0.5° resolution were produced based on relationships between chlorophyll contents, maximum electron transport rate and photosynthetic capacity (Alton, 2018). This is progress in the right direction given variations of maximum carboxylation rate in space-time; however, it requires thorough evaluations, not just during the peak growing season.

3.2.5. Tropical regions

Photosynthesis estimates in tropical forests are highly uncertain. In terms of incoming PAR and fraction of diffuse PAR, tropical regions showed the highest root mean squared error and positive bias in a MODIS-derived global land surface radiation product (Ryu et al., 2018). Higher cloud optical thickness, water vapor contents (Pinker and Laszlo, 1992), and less well known aerosol properties (Martin et al., 2010) result in imprecise mapping of PAR and diffuse PAR. There have been intensive debates in the community on remote sensing of the canopy structure in the tropics. A green-up of Amazon rainforests during the 2005 drought was reported using the MODIS EVI dataset (Saleska et al., 2007). However, this was contradicted by a study based on analysis of a dataset that excluded cloud-contaminated data, which did not show any green-up in 2005 (Samanta et al., 2010). Multiple papers reported green-up of Amazon rainforests during the dry season using MODIS LAI and EVI products (Brando et al., 2010; Huete et al., 2006; Myneni et al., 2007), but one study reported that variations of sun-sensor geometry, not vegetation, drove seasonal changes in EVI (Morton et al., 2014). To model seasonal variation of canopy photosynthesis in an Amazon rainforest site, it was essential to consider vertical variations in leaf photosynthetic capacity and leaf age with canopy depth (Wu et al., 2017). Several studies showed that photosynthetic capacity and leaf age could be estimated from leaf reflectance spectra (Chavana-Bryant et al., 2017; Dechant et al., 2017; Serbin et al., 2012). However, the hyperspectral data necessary for the large-scale estimation of these parameters is not yet available. Obtaining vertical variations of leaf traits in the canopy from remote sensing appears to be more challenging.

3.3. Relationships between SiF and photosynthesis

Over the last decade, linking SiF with canopy photosynthesis has received great attention. Particularly at regional to global scales, numerous papers have reported SiF as a good proxy for GPP (Frankenberg et al., 2011; Smith et al., 2018; Sun et al., 2017), and one paper reported a universal relationship between SiF from OCO2 and photosynthesis across various biomes (Li et al., 2018). However, field-based observations revealed diverse relationships between SiF and canopy photosynthesis within and between vegetation types (Damm et al., 2015; Yang et al., 2018b). It is therefore crucial to understand sources of uncertainties in relationships between SiF and photosynthesis at a range of scales.

To link SiF and canopy photosynthesis, it is useful to apply the LUE framework (Eq. (3)). Airborne and spaceborne instruments do not measure total emitted SiF, but only the SiF escaping from the canopy.

$$\mathrm{SiF} = \mathrm{APAR} \times \mathrm{LUE}_f \times f_{esc} \quad (3)$$

where $\mathrm{LUE_f}$ is the LUE of fluorescence of the whole canopy, and f_{esc} is the escape ratio, i.e., the fraction of escaping SiF relative to the total SiF emitted by the whole canopy. If we find a linear relationship between SiF and canopy photosynthesis, then there must be a linear relationship between LUE and $\mathrm{LUE}_f \times f_{esc}$. It is a great challenge, however, to tease out APAR and $\mathrm{LUE}_f \times f_{esc}$ from SiF observations (Porcar-Castell et al., 2014). While strong reabsorption of red SiF within canopy was well known, scattering of far-red SiF in the canopy was mostly neglected by assuming f_{esc} to be constant (Guanter et al., 2014). One reason for this was a lack of appropriate methods to estimate the term f_{esc}. Recent studies, however, provide reasonably simple formulae for this purpose and also indicate that f_{esc} can vary considerably over time and space (Yang and van der Tol, 2018). Together with the well-known fact that $\mathrm{LUE_f}$ varies little (Frankenberg and Berry, 2018), this implies that, somewhat counterintuitively, canopy structure effects might play a more important role in the SiF-GPP relationship than $\mathrm{LUE_f}$.

3.3.1. Canopy-scale

Relationships between SiF and canopy photosynthesis were found to vary with environmental variables and vegetation types. In a rice paddy, the temporal relationships between SiF and canopy photosynthesis differed across phenology, diffuse fraction of incoming light, and relative humidity at half-hourly temporal resolution (Yang et al., 2018b). Furthermore, a multiple regression model revealed that SiF was a very good proxy for APAR while containing little information on LUE, which does not support SiF as a proxy for canopy photosynthesis. In an airborne-based SiF study, the spatial relationships between SiF and

canopy photosynthesis differed between perennial grassland, cropland and mixed forest (Damm et al., 2015). Under severe heat stress situations, SiF was not able to track substantial reductions of canopy photosynthesis in an evergreen forest (Wohlfahrt et al., 2018) and a sugar beet site (Wieneke et al., 2018). A recent study linked f_{esc} with top-of-canopy reflectance under dense canopy conditions (Yang and van der Tol, 2018). Does the relationship between f_{esc}-corrected SiF (Eq. (3)) and canopy photosynthesis become linear and universal? Or does f_{esc}-corrected SiF show better correlation to APAR rather than canopy photosynthesis? Those questions must be addressed.

A robust scheme for up-scaling leaf-level SiF to the canopy scale is required to link SiF to flux tower-based canopy photosynthesis estimates. Footprints of SiF sensors depend on downward observation settings, which include view zenith angles such as nadir (Goulas et al., 2017) and off-nadir (Yang et al., 2015a), as well as fore-optics such as hemispheric with a cosine corrector (Yang et al., 2018b) and conical with bare fiber (Migliavacca et al., 2017). In a modeling study, a conical setting without cosine corrector only covered ~2% of flux tower footprint (Liu et al., 2017). Indeed, one study conducted in a mixed forest deployed a conical setting, which only covered three deciduous trees (~10 m^2), while the flux tower footprint covers more than 200 m^2, including both deciduous and evergreen species (Paul-Limoges et al., 2018). To fill the gaps in spatial scales, airborne SiF sensors such as HyPlant (Rascher et al., 2015) and CFIS (Frankenberg et al., 2018) might play key roles.

3.3.2. Regional and global scales

Satellite remote sensing of SiF, like conventional optical remote sensing of radiance and reflectance, is prone to errors from sensor degradation and requires careful investigation for sun-target-sensor geometry. SiF is radiance emitted from vegetation, not reflectance, so it is essential to keep precise absolute calibration of solar irradiance (Joiner et al., 2016). One study reported that in the 2015/2016 extreme drought period, Amazon forests showed reduction of SiF with increase in EVI, indicating decoupling of photosynthetic activity and greenness (Yang et al., 2018a). However, another study argued that the reduction of SiF in the Amazon forests was most likely driven by GOME2 sensor degradation (Zhang et al., 2018a) (also see Fig. 3). A recent study that compared OCO2-based SiF with the flux tower dataset identified a universal slope between SiF and canopy photosynthesis across diverse biomes except for C4 (Li et al., 2018), which is different from other studies that reported different slopes between SiF and canopy photosynthesis (Guanter et al., 2012). One study reanalyzed OCO2 SiF data by separating data into nadir, glint and target observation modes, which have different view zenith angles, and demonstrated that the slopes between SiF and photosynthesis varied with sun-target-sensor geometry (Zhang et al., 2018b).

Another important aspect of satellite SiF remote sensing is the retrieval noise in the signal and the corresponding limitations in temporal and spatial resolution. The GOME-2 SiF product (Joiner et al., 2013), for example, is available at 40 × 40 km resolution at three daily intervals, but is mostly used only in the form of monthly composites. This is partly due to spatial data gaps, but above all to the considerable level of noise in the signal, which can be reduced by temporal averaging. The OCO2 SiF product provides high spatial resolution (1.3 × 2.25 km) with 16 daily intervals, but its global sampling coverage is highly limited (Sun et al., 2017). The recently available SiF product from TROPOMI (Köhler et al., 2018) seems to overcome some of these limitations as the signal has a lower noise level than GOME-2, as well as almost daily global coverage with high spatial resolution (7 km × 3.5 km at nadir).

Is SiF good enough to estimate global photosynthesis? A recent study reported that NIRv, a proxy of NIR reflectance of vegetation, explained 90% of variations in GOME2 SiF over land globally on a monthly scale (Badgley et al., 2017). Furthermore, it showed that a machine learning-based global photosynthesis map (Beer et al., 2010) was better explained by MODIS-based NIRv (R^2 = 0.91) than by GOME2 SiF (R^2 = 0.73). Although higher spatial resolution in MODIS (500 m) than GOME-2 (40 km) partly explains the difference in predicting canopy photosynthesis, it is notable that the simple NIRv approach based on only two spectral bands could work as well as, or even better than, SiF for photosynthesis estimates. NIRv is mostly driven by canopy structure, rather than leaf physiology per se. Also, NIRv is reflectance-based and therefore does not contain any information on incoming radiation, which is required for successful estimation of photosynthesis at shorter time scales. SiF, in contrast, contains information on incoming radiation as well as vegetation properties. However, as fluorescence yield varies very little under various environmental and physiological conditions (Frankenberg and Berry, 2018; van der Tol et al., 2014), APAR and f_{esc} mainly determine SiF (Eq. (3)). We therefore assume that looking deeper into the relationships between APAR times f_{esc} and NIR reflectance (or radiance) from vegetation using the same satellite platform will help us identify the missing piece in linking SiF to canopy photosynthesis.

4. Opportunities

We are entering a phase of satellite remote sensing that offers unprecedented big data information in terms of spatial, temporal, and spectral domains. This will further advance our understanding of global photosynthesis estimates.

4.1. CubeSats

A CubeSat is a low-cost, miniaturized satellite that is composed of multiples of cubic units (10 by 10 by 10 cm). A constellation of more than 150 CubeSats operated by the company Planet Labs, Inc. (San Francisco, CA, USA) offers maps of red, green, blue and NIR channels at 3 m resolution, with daily revisit frequency over the entire globe (Hand, 2015). The key limitation was low spectral quality caused by wide ranges in spectral response of the four channels, and cross-CubeSat calibrations. A recent study overcame such limitations by integrating CubeSats, Landsat 8, and MODIS via a multi-scale machine learning technique to produce Landsat-like atmospherically corrected surface reflectance in the four channels while keeping the original spatial resolution and temporal revisit frequency of the CubeSat dataset (Houborg and McCabe, 2018b). These spectrally enhanced CubeSat data were then used to produce daily LAI and NDVI maps at 3 m resolution (Houborg and McCabe, 2018a). We expect that such high spatial and temporal resolution maps of LAI will play an important role in developing a robust upscaling scheme of photosynthesis from leaf to canopy, flux tower footprint and even coarser satellite pixels. It is notable that the number of CubeSats operated by other institutes, agencies and companies is increasing (https://www.nanosats.eu/) and it is feasible to include other spectral channels, which offer great potential for improving mapping of photosynthesis.

4.2. Geostationary satellites

The current generation of geostationary satellites such as GOES-16 and Himawari 8/9 provides multi-channel images at very high revisit frequency (~10 min) with a moderate spatial resolution (~1 km) (Bessho et al., 2016). This is particularly useful for tropical regions where frequent cloud cover prevents accurate retrievals of land surface properties and processes. Also, as those missions produce maps of atmospheric variables such as cloud and aerosol optical thicknesses, it will be possible to generate maps of solar radiation, PAR and diffuse PAR at the land surface with high temporal resolution, which could be directly coupled to the land surface variables to compute photosynthesis. So far, global remote sensing of photosynthesis has relied on at most one or two snapshots per day, and upscaled them to the daily scales with simple cosine functions (Frankenberg et al., 2011; Ryu et al.,

2012). Sub-daily monitoring of vegetation status could lead to detection of plant water stress earlier and more accurately (Chaves et al., 2002). Integration of multiple geostationary satellites across different continents could open new opportunities to track diurnal variations of photosynthesis at the global scale. Also, several planned geostationary missions such as GeoCarb and TEMPO aim to produce moderate spatial resolution, sub-daily SiF maps at continental scales (Zoogman et al., 2017), which will be instrumental for photosynthesis monitoring.

4.3. Hyperspectral satellites

One important report that will shape the next decadal strategy for Earth monitoring from space by NASA, NOAA and USGS particularly stressed the importance, significance and urgency of hyperspectral satellite remote sensing (National Academies of Sciences and Medicine, 2018). Hyperspectral remote sensing missions at global scale are currently under development such as EnMAP, HyspIRI, PRISMA and FLEX. The planned missions will provide rich information for vegetation photosynthetic processes and enable us to apply statistical methods such as machine learning and multivariate regression to retrieve photosynthetic capacity and leaf traits that were already achieved from airborne remote sensing (Asner et al., 2015; Serbin et al., 2015). Combining hyperspectral reflectance maps with FLUXNET-based canopy photosynthesis datasets could also enable direct estimations of photosynthesis across diverse ecosystems (DuBois et al., 2018). The suitability of TROPOMI data for SiF retrieval at higher spatial and temporal resolutions than previous SiF products was already demonstrated (Köhler et al., 2018), and the FLEX mission will provide the possibility to retrieve the full SiF emission spectrum from red to far-red regions at finer spatial resolution (300 m) (Drusch et al., 2017).

4.4. Hotspots

Hotspots in vegetation, which are seen when target, sensor, and the Sun are aligned, offer key information for quantifying canopy structure and bidirectional reflectance factor (Jupp and Strahler, 1991). However, previous satellites were not able to monitor hotspots only given the various phase angles with Sun-target-sensor geometries. The EPIC sensor onboard the DSCOVR spacecraft is located in the L1 Lagrangian point (1.5 million km from the Earth towards the Sun), where it only sees the sunlit side of the full disc of Earth every two hours (Marshak et al., 2018). Given the position of the satellite at the L1 point, we could minimize the angular variations of surface reflectance as the phase angle is near 0. The EPIC dataset will be useful for understanding variations in vegetation reflectance and indices in the Amazon rainforests, which have been debated intensively (Morton et al., 2014; Samanta et al., 2010). Furthermore, it will provide unique opportunities for quantifying canopy structure better at global scales. For example, a recent paper showed global maps of LAI and its sunlit fraction based on EPIC data (Yang et al., 2017).

4.5. Integration

There is not a silver bullet for global photosynthesis estimates. With the new opportunities, we will have to integrate different data sources and approaches to overcome the uncertainties summarized in Section 3. In particular, image fusion across spatial, temporal and spectral domains with multiple satellites could maximize strengths from individual satellite data (Gao et al., 2006; Houborg and McCabe, 2018b). To do so, the key to success will be efficient use of computational resources given the rapid increase in size of earth observation data. Several platforms are already available, including the Google Earth Engine (Gorelick et al., 2017), NASA Earth Exchange (Nemani et al., 2011), and other cloud computing services (Agarwal et al., 2011). With more overlap in the data from multiple remote sensing datasets in terms of space, time and spectral responses, developing consistent, cross-calibrated, long-term vegetation structure and functional maps is a key priority as this could help quantify interannual variations and trends of global photosynthesis, which are highly uncertain. Last but not least, it is important to revisit the theories developed in the past and integrate them into emerging big data analysis to understand global photosynthesis better.

5. Conclusion

In the Introduction, we raised the question: how much have we advanced global photosynthesis research since the Photosynthesis and Production Workshop held in Trebon, 1969? We argue that most important theories, observations and modeling, though not conducted at a global scale, had been conceived before the workshop. Since then, key advances have been made in preparing input data and constraining parameters better for photosynthesis models from satellite remote sensing across Landsat, AVHRR, MODIS, and many other platforms with historical contexts such as the missing carbon debate and EOS program. In terms of C. T. de Wit's concern for garbage-in, garbage-out stated at the 1969 workshop, we now have an abundance of high-quality forcing data for photosynthesis models via satellite remote sensing, but we have to remember his concerns as we see large discrepancies in global photosynthesis estimates based on different forcing data and models (Fig. 3). To advance global photosynthesis research, priority must be given to improving the quantity and quality of data on PAR, canopy structure such as LAI, clumping index and leaf angle distribution, LUE model forcings and structure that considers water stress and CO_2 fertilization effects better, and clarifying SiF and canopy photosynthesis relationships. It is also important to recognize that it is impossible to verify and validate numerical models of natural systems which are never closed (Oreskes et al., 1994), which is the case of global photosynthesis estimate. Therefore, integration of model hierarchy, scaling and multiple constraints to closure from top down estimates is essential. Understanding old theories and models in depth, incorporating emergent big datasets from satellite constellations, and evaluating and constraining photosynthesis models with extensive in-situ spectral, leaf trait, and flux tower data will lead us to improve global estimates of photosynthesis.

Acknowledgements

We appreciate all the great scientists whose achievements over multiple decades have enabled us to write this review. We thank Richard Waring, Tiit Nilson, John Norman, Steve Running and late Paul Jarvis for sharing history of photosynthesis and canopy structure studies. We thank Benjamin Dechant for internal review, Chongya Jiang for processing the GPP dataset, Remi Luo for sharing global SiF time series from his paper, Yorum Hwang for making Fig. 2, and John Gamon for sharing his opinion on PRI. YR was supported by the National Research Foundation of Korea (NRF-2016M1A3A3A02018195). Proofreading service was supported by the Research Institute of Agriculture and Life Sciences at SNU. While initiating this paper during sabbatical leave, YR was supported by the Carnegie Institution for Science. DDB is supported by the Department of Energy, Biological and Environmental Research, which funds the AmeriFlux program, and by the California Agricultural Experiment Station, McIntire-Stennis Project of the United States Department of Agriculture.

References

Agarwal, D., Cheah, Y.-W., Fay, D., Fay, J., Guo, D., Hey, T., Humphrey, M., Jackson, K., Li, Jie, Poulain, C., Ryu, Y., van Ingen, C., 2011. Data-intensive science: the Terapixel and MODISAzure projects. Int. J. High Perform. Comput. Appl. 25, 304–316.

Alemohammad, S.H., Fang, B., Konings, A.G., Aires, F., Green, J.K., Kolassa, J., Miralles, D., Prigent, C., Gentine, P., 2017. Water, Energy, and Carbon with Artificial Neural Networks (WECANN): a statistically based estimate of global surface turbulent fluxes and gross primary productivity using solar-induced fluorescence. Biogeosciences 14, 4101–4124.

Ali, A.A., Xu, C., Rogers, A., McDowell, N.G., Medlyn, B.E., Fisher, R.A., Wullschleger, S.D., Reich, P.B., Vrugt, J.A., Bauerle, W.L., Santiago, L.S., Wilson, C.J., 2015. Global-scale environmental control of plant photosynthetic capacity. Ecol. Appl. 25, 2349–2365.

Alton, P.B., 2017. Retrieval of seasonal Rubisco-limited photosynthetic capacity at global FLUXNET sites from hyperspectral satellite remote sensing: impact on carbon modelling. Agric. For. Meteorol. 232, 74–88.

Alton, P.B., 2018. Decadal trends in photosynthetic capacity and leaf area index inferred from satellite remote sensing for global vegetation types. Agric. For. Meteorol. 250–251, 361–375.

Anav, A., Friedlingstein, P., Beer, C., Ciais, P., Harper, A., Jones, C., Murray-Tortarolo, G., Papale, D., Parazoo, N.C., Peylin, P., Piao, S., Sitch, S., Viovy, N., Wiltshire, A., Zhao, M., 2015. Spatiotemporal patterns of terrestrial gross primary production: a review. Rev. Geophys. 53, 785–818.

André, J.-C., Goutorbe, J.-P., Perrier, A., 1986. HAPEX—MOBILHY: a hydrologic atmospheric experiment the study of water budget and evaporation flux at the climatic scale. Bull. Am. Meteorol. Soc. 67, 138–144.

Asner, G.P., Martin, R.E., Knapp, D.E., Tupayachi, R., Anderson, C., Carranza, L., Martinez, P., Houcheime, M., Sinca, F., Weiss, P., 2011. Spectroscopy of canopy chemicals in humid tropical forests. Remote Sens. Environ. 115, 3587–3598.

Asner, G.P., Martin, R.E., Anderson, C.B., Knapp, D.E., 2015. Quantifying forest canopy traits: imaging spectroscopy versus field survey. Remote Sens. Environ. 158, 15–27.

Asrar, G., Dokken, D.J., 1993. EOS Reference Handbook. NASA, Greenbelt, MD.

Aubinet, M., Grelle, A., Ibrom, A., Rannik, U., Moncrieff, J., Foken, T., Kowalski, A.S., Martin, P.H., Berbigier, P., Bernhofer, C., Clement, R., Elbers, J., Granier, A., Grunwald, T., Morgenstern, K., Pilegaard, K., Rebmann, C., Snijders, W., Valentini, R., Vesala, T., 2000. Estimates of the annual net carbon and water exchange of forests: the EUROFLUX methodology. Adv. Ecol. Res. 30, 113–175.

Badgley, G., Field, C.B., Berry, J.A., 2017. Canopy near-infrared reflectance and terrestrial photosynthesis. Sci. Adv. 3, e1602244.

Bailey, B.N., Mahaffee, W.F., 2017. Rapid measurement of the three-dimensional distribution of leaf orientation and the leaf angle probability density function using terrestrial LiDAR scanning. Remote Sens. Environ. 194, 63–76.

Baldocchi, D., 2014. Measuring fluxes of trace gases and energy between ecosystems and the atmosphere - the state and future of the eddy covariance method. Glob. Chang. Biol. 20, 3600–3609.

Baldocchi, D., Meyers, T., 1998. On using eco-physiological, micrometeorological and biogeochemical theory to evaluate carbon dioxide, water vapor and trace gas fluxes over vegetation: a perspective. Agric. For. Meteorol. 90, 1–25.

Baldocchi, D., Penuelas, J., 2019. The physics and ecology of mining carbon dioxide from the atmosphere by ecosystems. Glob. Chang. Biol. https://doi.org/10.1111/gcb.14559.

Baldocchi, D.D., Verma, S.B., Anderson, D.E., 1987. Canopy photosynthesis and water-use efficiency in a deciduous forest. J. Appl. Ecol. 24, 251–260.

Baldocchi, D., Valentini, R., Running, S., Oechel, W., Dahlman, R., 1996. Strategies for measuring and modelling carbon dioxide and water vapour fluxes over terrestrial ecosystems. Glob. Chang. Biol. 2, 159–168.

Baldocchi, D., Falge, E., Gu, L.H., Olson, R., Hollinger, D., Running, S., Anthoni, P., Bernhofer, C., Davis, K., Evans, R., Fuentes, J., Goldstein, A., Katul, G., Law, B., Lee, X.H., Malhi, Y., Meyers, T., Munger, W., Oechel, W., Paw, U., K., T., Pilegaard, K., Schmid, H.P., Valentini, R., Verma, S., Vesala, T., Wilson, K., Wofsy, S., 2001. FLUXNET: a new tool to study the temporal and spatial variability of ecosystem-scale carbon dioxide, water vapor, and energy flux densities. Bull. Am. Meteorol. Soc. 82, 2415–2434.

Ball, J.T., Woodrow, I.E., Berry, J.A., 1987. A model predicting stomatal conductance and its contribution to the control of photosynthesis under different environmental conditions. In: Biggins, J. (Ed.), Progress in Photosynthesis Research: Volume 4 Proceedings of the 7th International Congress on Photosynthesis Providence, Rhode Island, USA, August 10–15, 1986. Springer Netherlands, Dordrecht, pp. 221–224.

Baret, F., Hagolle, O., Geiger, B., Bicheron, P., Miras, B., Huc, M., Berthelot, B., Nino, F., Weiss, M., Samain, O., Roujean, J.L., Leroy, M., 2007. LAI, fAPAR and fCover CYCLOPES global products derived from VEGETATION - part 1: principles of the algorithm. Remote Sens. Environ. 110, 275–286.

Bate, G.C., Canvin, D.T., 1971. A gas-exchange system for measuring the productivity of plant populations in controlled environments. Can. J. Bot. 49, 601–608.

Bauer, M.E., Daughtry, C.S.T., Biehl, L.L., Kanemasu, E.T., Hall, F.G., 1986. Field spectroscopy of agricultural crops. IEEE Trans. Geosci. Remote Sens. GE-24, 65–75.

Baumgartner, A., 1969. Meteorological approach to the exchange of CO_2 between the atmosphere and vegetation, particularly forest stands. Photosynthetica 3, 27–149.

Beer, C., Reichstein, M., Tomelleri, E., Ciais, P., Jung, M., Carvalhais, N., Rodenbeck, C., Arain, M.A., Baldocchi, D., Bonan, G.B., Bondeau, A., Cescatti, A., Lasslop, G., Lindroth, A., Lomas, M., Luyssaert, S., Margolis, H., Oleson, K.W., Roupsard, O., Veenendaal, E., Viovy, N., Williams, C., Woodward, F.I., Papale, D., 2010. Terrestrial gross carbon dioxide uptake: global distribution and covariation with climate. Science 329, 834–838.

Bessho, K., Date, K., Hayashi, M., Ikeda, A., Imai, T., Inoue, H., Kumagai, Y., Miyakawa, T., Murata, H., Ohno, T., Okuyama, A., Oyama, R., Sasaki, Y., Shimazu, Y., Shimoji, K., Sumida, Y., Suzuki, M., Taniguchi, H., Tsuchiyama, H., Uesawa, D., Yokota, H., Yoshida, R., 2016. An introduction to himawari-8/9 - Japan's new-generation geostationary meteorological satellites. J. Meteorol. Soc. Jpn. 94, 151–183.

Billings, W.D., Morris, R.J., 1951. Reflection of visible and infrared radiation from leaves of different ecological groups. Am. J. Bot. 38, 327–331.

Billings, W.D., Clebsch, E.E.C., Mooney, H.A., 1961. Effect of low concentrations of carbon dioxide on photosynthesis rates of two races of oxyria. Science 133, 1834.

Björkman, O., 1966. The effect of oxygen concentration on photosynthesis in higher plants. Physiol. Plant. 19, 618–633.

Björkman, O., Holmgren, P., 1963. Adaptability of the photosynthetic apparatus to light intensity in ecotypes from exposed and shaded habitats. Physiol. Plant. 16, 889–914.

Black, T.A., DenHartog, G., Neumann, H.H., Blanken, P.D., Yang, P.C., Russell, C., Nesic, Z., Lee, X., Chen, S.G., Staebler, R., Novak, M.D., 1996. Annual cycles of water vapour and carbon dioxide fluxes in and above a boreal aspen forest. Glob. Chang. Biol. 2, 219–229.

Bodesheim, P., Jung, M., Gans, F., Mahecha, M.D., Reichstein, M., 2018. Upscaled diurnal cycles of land–atmosphere fluxes: a new global half-hourly data product. Earth Syst. Sci. Data 10, 1327–1365.

Bolin, B., 1977. Changes of land biota and their importance for the carbon cycle. Science 196, 613–615.

Bolin, B., Keeling, C.D., 1963. Large-scale atmospheric mixing as deduced from the seasonal and meridional variations of carbon dioxide. J. Geophys. Res. 68, 3899–3920.

Bonan, G.B., Lawrence, P.J., Oleson, K.W., Levis, S., Jung, M., Reichstein, M., Lawrence, D.M., Swenson, S.C., 2011. Improving canopy processes in the Community Land Model version 4 (CLM4) using global flux fields empirically inferred from FLUXNET data. J. Geophys. Res. 116. https://doi.org/10.1029/2010jg001593.

Bonan, G.B., Oleson, K.W., Fisher, R.A., Lasslop, G., Reichstein, M., 2012. Reconciling leaf physiological traits and canopy flux data: use of the TRY and FLUXNET databases in the Community Land Model version 4. J. Geophys. Res. Biogeosci. 117. https://doi.org/10.1029/2011JG001913.

Bowes, G., Ogren, W.L., Hageman, R.H., 1971. Phosphoglycolate production catalyzed by ribulose diphosphate carboxylase. Biochem. Biophys. Res. Commun. 45, 716–722.

Brando, P.M., Goetz, S.J., Baccini, A., Nepstad, D.C., Beck, P.S.A., Christman, M.C., 2010. Seasonal and interannual variability of climate and vegetation indices across the Amazon. Proc. Natl. Acad. Sci. U. S. A. 107, 14685–14690.

Broecker, W.S., Takahashi, T., Simpson, H.J., Peng, T.-H., 1979. Fate of fossil fuel carbon dioxide and the global carbon budget. Science 206, 409–418.

Brown, K.W., Rosenberg, N.J., 1971. Energy and CO_2 balance of an irrigated sugar beet (*Beta vulgaris*) field in the great plains1. Agron. J. 63, 207–213.

Calvin, M., Benson, A.A., 1948. The path of carbon in photosynthesis. Science 107, 476–480.

Chavana-Bryant, C., Malhi, Y., Wu, J., Asner, G.P., Anastasiou, A., Enquist, B.J., Cosio Caravasi, E.G., Doughty, C.E., Saleska, S.R., Martin, R.E., Gerard, F.F., 2017. Leaf aging of Amazonian canopy trees as revealed by spectral and physiochemical measurements. New Phytol. 214, 1049–1063.

Chaves, M.M., Pereira, J.S., Maroco, J., Rodrigues, M.L., Ricardo, C.P.P., OsÓRio, M.L., Carvalho, I., Faria, T., Pinheiro, C., 2002. How plants cope with water stress in the field? Photosynthesis and growth. Ann. Bot. 89, 907–916.

Chen, J.M., Liu, J., Cihlar, J., Goulden, M.L., 1999. Daily canopy photosynthesis model through temporal and spatial scaling for remote sensing applications. Ecol. Model. 124, 99–119.

Chen, J.M., Menges, C.H., Leblanc, S.G., 2005. Global mapping of foliage clumping index using multi-angular satellite data. Remote Sens. Environ. 97, 447–457.

Chu, H., Baldocchi, D.D., John, R., Wolf, S., Reichstein, M., 2017. Fluxes all of the time? A primer on the temporal representativeness of FLUXNET. J. Geophys. Res. Biogeosci. 122, 289–307.

Ciais, P., Tans, P.P., Trolier, M., White, J.W.C., Francey, R.J., 1995. A large northern hemisphere terrestrial CO_2 sink indicated by the $^{13}C/^{12}C$ ratio of atmospheric CO_2. Science 269, 1098–1102.

Collatz, G.J., Ball, J.T., Grivet, C., Berry, J.A., 1991. Physiological and environmental regulation of stomatal conductance, photosynthesis and transpiration: a model that includes a laminar boundary layer. Agric. For. Meteorol. 54, 107–136.

Collatz, G.J., Ribas-Carbo, M., Berry, J.A., 1992. Coupled photosynthesis-stomatal conductance model for leaves of C4 plants. Aust. J. Plant Physiol. 19, 519–538.

Coops, N.C., Hilker, T., Hall, F.G., Nichol, C.J., Drolet, G.G., 2010. Estimation of light-use efficiency of terrestrial ecosystems from space: a status report. Bioscience 60, 788–797.

Croft, H., Chen, J.M., Luo, X., Bartlett, P., Chen, B., Staebler, R.M., 2017. Leaf chlorophyll content as a proxy for leaf photosynthetic capacity. Glob. Chang. Biol. 23, 3513–3524.

Curran, P.J., 1989. Remote sensing of foliar chemistry. Remote Sens. Environ. 30, 271–278.

Curtis, O.F., 1936. Leaf temperatures and the cooling of leaves by radiation. Plant Physiol. 11, 343–364.

Damm, A., Guanter, L., Paul-Limoges, E., van der Tol, C., Hueni, A., Buchmann, N., Eugster, W., Ammann, C., Schaepman, M.E., 2015. Far-red sun-induced chlorophyll fluorescence shows ecosystem-specific relationships to gross primary production: an assessment based on observational and modeling approaches. Remote Sens. Environ. 166, 91–105.

De Wit, C.T., 1959. Potential photosynthesis of crop surfaces. Neth. J. Agric. Sci. 7, 141–149.

de Wit, C.T., 1965. Photosynthesis of Leaf Canopies. Wageningen.

de Wit, C.T., 1970. Dynamic concepts in biology. In: Malek, I. (Ed.), Prediction and Measurement of Photosynthetic Productivity. Proceeding IBP/PP Technical Meeting, Trebon, Czech. Centre for Agricultural Publishing and Documentation, Wageningen, The Netherlands, pp. 17–23.

Dechant, B., Cuntz, M., Vohland, M., Schulz, E., Doktor, D., 2017. Estimation of photosynthesis traits from leaf reflectance spectra: correlation to nitrogen content as the dominant mechanism. Remote Sens. Environ. 196, 279–292.

Demarty, J., Chevallier, F., Friend, A.D., Viovy, N., Piao, S., Ciais, P., 2007. Assimilation of global MODIS leaf area index retrievals within a terrestrial biosphere model. Geophys. Res. Lett. 34. https://doi.org/10.1029/2007GL030014.

Denmead, O.T., Bradley, E.F., 1985. Flux-gradient relationships in a forest canopy. In: Hutchison, B.A., Hicks, B.B. (Eds.), The Forest-Atmosphere Interaction: Proceedings of the Forest Environmental Measurements Conference Held at Oak Ridge, Tennessee,

October 23–28, 1983. Springer Netherlands, Dordrecht, pp. 421–442.
Drolet, G.G., Middleton, E.M., Huemmrich, K.F., Hall, F.G., Amiro, B.D., Barr, A.G., Black, T.A., McCaughey, J.H., Margolis, H.A., 2008. Regional mapping of gross light-use efficiency using MODIS spectral indices. Remote Sens. Environ. 112, 3064–3078.
Drusch, M., Moreno, J., Bello, U.D., Franco, R., Goulas, Y., Huth, A., Kraft, S., Middleton, E.M., Miglietta, F., Mohammed, G., Nedbal, L., Rascher, U., Schüttemeyer, D., Verhoef, W., 2017. The FLuorescence EXplorer mission concept—ESA's earth explorer 8. IEEE Trans. Geosci. Remote Sens. 55, 1273–1284.
DuBois, S., Desai, A.R., Singh, A., Serbin, S.P., Goulden, M.L., Baldocchi, D.D., Ma, S., Oechel, W.C., Wharton, S., Kruger, E.L., Townsend, P.A., 2018. Using imaging spectroscopy to detect variation in terrestrial ecosystem productivity across a water-stressed landscape. Ecol. Appl. 28, 1313–1324.
Duncan, W., Loomis, R., Williams, W., Hanau, R., 1967. A model for simulating photosynthesis in plant communities. Hilgardia 38, 181–205.
Ebermayer, E.W.F., 1982. Naturgesetzliche Grundlagen des Wald-undAckerbaues. Pt. I: Physiologische Chemie der Pflanzen, Vol. 1: Die Bestandtheile der Pflanzen. Springer, Berlin.
Eckardt, F.E., 1968. Techniques de mesure de la photosynthese sur le terrain basees dur l'emploi d'enceintes climatisees. In: Eckardt, F.E. (Ed.), Functioning of Terrestrial Ecosystems at the Primary Production Level. UNESCO, Paris, pp. 289–319.
Ehleringer, J., Bjorkman, O., 1977. Quantum yields for CO_2 uptake in C3 and C4 plants-dependence on temperature, CO_2, and O_2 concentration. Plant Physiol. 59, 86–90.
Entekhabi, D., Njoku, E.G., Neill, P.E.O., Kellogg, K.H., Crow, W.T., Edelstein, W.N., Entin, J.K., Goodman, S.D., Jackson, T.J., Johnson, J., Kimball, J., Piepmeier, J.R., Koster, R.D., Martin, N., McDonald, K.C., Moghaddam, M., Moran, S., Reichle, R., Shi, J.C., Spencer, M.W., Thurman, S.W., Tsang, L., Zyl, J.V., 2010. The soil moisture active passive (SMAP) mission. Proc. IEEE 98, 704–716.
Enting, I.G., Mansbridge, J.V., 1991. Latitudinal distribution of sources and sinks of CO_2: results of an inversion study. Tellus Ser. B Chem. Phys. Meteorol. 43, 156–170.
Fang, H., Wei, S., Jiang, C., Scipal, K., 2012. Theoretical uncertainty analysis of global MODIS, CYCLOPES, and GLOBCARBON LAI products using a triple collocation method. Remote Sens. Environ. 124, 610–621.
Farquhar, G.D., 1979. Models describing the kinetics of ribulose biphosphate carboxylase-oxygenase. Arch. Biochem. Biophys. 193, 456–468.
Farquhar, G.D., von Caemmerer, S., Berry, J.A., 1980. A biochemical model of photosynthetic CO_2 assimilation in leaves of C_3 species. Planta 149, 78–90.
Field, C., Mooney, H.A., 1986. The photosynthesis-nitrogen relationship in wild plants. In: Givnish, T.J. (Ed.), On the Economy of Plant Form and Function. Cambridge University Press, pp. 25–55.
Filella, I., Porcar-Castell, A., Munné-Bosch, S., Bäck, J., Garbulsky, M.F., Peñuelas, J., 2009. PRI assessment of long-term changes in carotenoids/chlorophyll ratio and short-term changes in de-epoxidation state of the xanthophyll cycle. Int. J. Remote Sens. 30, 4443–4455.
Foley, J.A., 1994. Net primary productivity in the terrestrial biosphere: the application of a global model. J. Geophys. Res.-Atmos. 99, 20773–20783.
Frankenberg, C., Berry, J., 2018. 3.10 - solar induced chlorophyll fluorescence: origins, relation to photosynthesis and retrieval A2 - Liang, Shunlin. In: Comprehensive Remote Sensing. Elsevier, Oxford, pp. 143–162.
Frankenberg, C., Fisher, J.B., Worden, J., Badgley, G., Saatchi, S.S., Lee, J.-E., Toon, G.C., Butz, A., Jung, M., Kuze, A., Yokota, T., 2011. New global observations of the terrestrial carbon cycle from GOSAT: patterns of plant fluorescence with gross primary productivity. Geophys. Res. Lett. 38. https://doi.org/10.1029/2011GL048738.
Frankenberg, C., Köhler, P., Magney, T.S., Geier, S., Lawson, P., Schwochert, M., McDuffie, J., Drewry, D.T., Pavlick, R., Kuhnert, A., 2018. The Chlorophyll Fluorescence Imaging Spectrometer (CFIS), mapping far red fluorescence from aircraft. Remote Sens. Environ. 217, 523–536.
Friedl, M.A., Sulla-Menashe, D., Tan, B., Schneider, A., Ramankutty, N., Sibley, A., Huang, X., 2010. MODIS collection 5 global land cover: algorithm refinements and characterization of new datasets. Remote Sens. Environ. 114, 168–182.
Fung, I., Prentice, K., Matthews, E., Lerner, J., Russell, G., 1983. Three-dimensional tracer model study of atmospheric CO_2: response to seasonal exchanges with the terrestrial biosphere. J. Geophys. Res. Oceans 88, 1281–1294.
Gaastra, P., 1959. Photosynthesis of Crop Plants as Influenced by Light, Carbon Dioxide, Temperature, and Stomatal Diffusion Resistance. Veenman, Wageningen.
Gabrielsen, E.K., 1949. Photosynthesis in leaves at very low carbon dioxide concentrations. Nature 163, 359.
Gamon, J.A., Penuelas, J., Field, C.B., 1992. A narrow-waveband spectral index that tracks diurnal changes in photosynthetic efficiency. Remote Sens. Environ. 41, 35–44.
Gamon, J.A., Huemmrich, K.F., Wong, C.Y.S., Ensminger, I., Garrity, S., Hollinger, D.Y., Noormets, A., Peñuelas, J., 2016. A remotely sensed pigment index reveals photosynthetic phenology in evergreen conifers. Proc. Natl. Acad. Sci. 113, 13087–13092.
Gao, B.-C., 1996. NDWI-A Normalized Difference Water Index for remote sensing of vegetation liquid water from space. Remote Sens. Environ. 58, 257–266.
Gao, F., Masek, J., Schwaller, M., Hall, F., 2006. On the blending of the Landsat and MODIS surface reflectance: predicting daily Landsat surface reflectance. IEEE Trans. Geosci. Remote Sens. 44, 2207–2218.
Garbulsky, M.F., Peñuelas, J., Papale, D., Ardö, J., Goulden, M.L., Kiely, G., Richardson, A.D., Rotenberg, E., Veenendaal, E.M., Filella, I., 2010. Patterns and controls of the variability of radiation use efficiency and primary productivity across terrestrial ecosystems. Glob. Ecol. Biogeogr. 19, 253–267.
Garbulsky, M.F., Peñuelas, J., Gamon, J., Inoue, Y., Filella, I., 2011. The photochemical reflectance index (PRI) and the remote sensing of leaf, canopy and ecosystem radiation use efficiencies: a review and meta-analysis. Remote Sens. Environ. 115, 281–297.
Gates, D.M., 1968. Transpiration and leaf temperature. Annu. Rev. Plant Physiol. 19, 211–238.
Gates, D.M., Tantraporn, W., 1952. The reflectivity of deciduous trees and herbaceous plants in the infrared to 25 microns. Science 115, 613–616.
Gates, D.M., Keegan, H.J., CSchleter, J.C., Weidner, V.R., 1965. Spectral properties of plants. Appl. Opt. 4, 11–20.
Gentine, P., Alemohammad, S.H., 2018. Reconstructed solar-induced fluorescence: a machine learning vegetation product based on MODIS surface reflectance to reproduce GOME-2 solar-induced fluorescence. Geophys. Res. Lett. 45, 3136–3146.
Genty, B., Briantais, J.-M., Baker, N.R., 1989. The relationship between the quantum yield of photosynthetic electron transport and quenching of chlorophyll fluorescence. Biochim. Biophys. Acta Gen. Subj. 990, 87–92.
Gong, P., Wang, J., Yu, L., Zhao, Y., Zhao, Y., Liang, L., Niu, Z., Huang, X., Fu, H., Liu, S., Li, C., Li, X., Fu, W., Liu, C., Xu, Y., Wang, X., Cheng, Q., Hu, L., Yao, W., Zhang, H., Zhu, P., Zhao, Z., Zhang, H., Zheng, Y., Ji, L., Zhang, Y., Chen, H., Yan, A., Guo, J., Yu, L., Wang, L., Liu, X., Shi, T., Zhu, M., Chen, Y., Yang, G., Tang, P., Xu, B., Giri, C., Clinton, N., Zhu, Z., Chen, J., Chen, J., 2013. Finer resolution observation and monitoring of global land cover: first mapping results with Landsat TM and ETM+ data. Int. J. Remote Sens. 34, 2607–2654.
Gorelick, N., Hancher, M., Dixon, M., Ilyushchenko, S., Thau, D., Moore, R., 2017. Google earth engine: planetary-scale geospatial analysis for everyone. Remote Sens. Environ. 202, 18–27.
Goudriaan, J., 1977. Crop Micrometeorology: A Simulation Study. Pudoc, Wageningen.
Goulas, Y., Fournier, A., Daumard, F., Champagne, S., Ounis, A., Marloie, O., Moya, I., 2017. Gross primary production of a wheat canopy relates stronger too far red than to red solar-induced chlorophyll fluorescence. Remote Sens. 9, 97.
Goward, S.N., Tucker, C.J., Dye, D.G., 1985. North American vegetation patterns observed with the NOAA-7 advanced very high resolution radiometer. Vegetatio 64, 3–14.
Goward, S.N., Markham, B., Dye, D.G., Dulaney, W., Yang, J., 1991. Normalized difference vegetation index measurements from the advanced very high resolution radiometer. Remote Sens. Environ. 35, 257–277.
Guanter, L., Alonso, L., Gomez-Chova, L., Amoros-Lopez, J., Vila, J., Moreno, J., 2007. Estimation of solar-induced vegetation fluorescence from space measurements. Geophys. Res. Lett. 34. https://doi.org/10.1029/2007GL029289.
Guanter, L., Frankenberg, C., Dudhia, A., Lewis, P.E., Gómez-Dans, J., Kuze, A., Suto, H., Grainger, R.G., 2012. Retrieval and global assessment of terrestrial chlorophyll fluorescence from GOSAT space measurements. Remote Sens. Environ. 121, 236–251.
Guanter, L., Zhang, Y., Jung, M., Joiner, J., Voigt, M., Berry, J.A., Frankenberg, C., Huete, A.R., Zarco-Tejada, P., Lee, J.-E., Moran, M.S., Ponce-Campos, G., Beer, C., Camps-Valls, G., Buchmann, N., Gianelle, D., Klumpp, K., Cescatti, A., Baker, J.M., Griffis, T.J., 2014. Global and time-resolved monitoring of crop photosynthesis with chlorophyll fluorescence. Proc. Natl. Acad. Sci. 111, E1327–E1333.
Gurney, K.R., Baker, D., Rayner, P., Denning, S., 2008. Interannual variations in continental-scale net carbon exchange and sensitivity to observing networks estimated from atmospheric CO_2 inversions for the period 1980 to 2005. Glob. Biogeochem. Cycles 22.
Hall, A.E., 1979. A model of leaf photosynthesis and respiration for predicting carbon dioxide assimilation in different environments. Oecologia 43, 299–316.
Hall, F.G., Hilker, T., Coops, N.C., 2012. Data assimilation of photosynthetic light-use efficiency using multi-angular satellite data: I. Model formation. Remote Sens. Environ. 121, 301–308.
Hand, E., 2015. Startup liftoff. Science 348, 172–177.
Hansen, M.C., Potapov, P.V., Moore, R., Hancher, M., Turubanova, S.A., Tyukavina, A., Thau, D., Stehman, S.V., Goetz, S.J., Loveland, T.R., Kommareddy, A., Egorov, A., Chini, L., Justice, C.O., Townshend, J.R.G., 2013. High-resolution global maps of 21st-century forest cover change. Science 342, 850–853.
Hatch, M., Slack, C., 1966. Photosynthesis by sugar-cane leaves. A new carboxylation reaction and the pathway of sugar formation. Biochem. J. 101, 103–111.
Haxeltine, A., Prentice, I.C., 1996a. BIOME3: an equilibrium terrestrial biosphere model based on ecophysiological constraints, resource availability, and competition among plant functional types. Glob. Biogeochem. Cycles 10, 693–709.
Haxeltine, A., Prentice, I.C., 1996b. A general model for the light-use efficiency of primary production. Funct. Ecol. 10, 551–561.
Heimann, M., Keeling, C.D., 1989. A three-dimensional model of atmospheric CO_2 transport based on observed winds: 2. Model description and simulated tracer experiments. In: Peterson, D.H. (Ed.), Aspects of Climate Variability in the Pacific and the Western Americas. American Geophysical Union, Washington, DC, pp. 237–274.
Heimann, M., Reichstein, M., 2008. Terrestrial ecosystem carbon dynamics and climate feedbacks. Nature 451, 289–292.
Heinsch, F.A., Zhao, M.S., Running, S.W., Kimball, J.S., Nemani, R.R., Davis, K.J., Bolstad, P.V., Cook, B.D., Desai, A.R., Ricciuto, D.M., Law, B.E., Oechel, W.C., Kwon, H., Luo, H.Y., Wofsy, S.C., Dunn, A.L., Munger, J.W., Baldocchi, D.D., Xu, L.K., Hollinger, D.Y., Richardson, A.D., Stoy, P.C., Siqueira, M.B.S., Monson, R.K., Burns, S.P., Flanagan, L.B., 2006. Evaluation of remote sensing based terrestrial productivity from MODIS using regional tower eddy flux network observations. IEEE Trans. Geosci. Remote Sens. 44, 1908–1925.
Hilker, T., Coops, N.C., Wulder, M.A., Black, T.A., Guy, R.D., 2008. The use of remote sensing in light use efficiency based models of gross primary production: a review of current status and future requirements. Sci. Total Environ. 404, 411–423.
Hilker, T., Lyapustin, A., Hall, F.G., Wang, Y., Coops, N.C., Drolet, G., Black, T.A., 2009. An assessment of photosynthetic light use efficiency from space: modeling the atmospheric and directional impacts on PRI reflectance. Remote Sens. Environ. 113, 2463–2475.
Hmimina, G., Merlier, E., DufrêNe, E., Soudani, K., 2015. Deconvolution of pigment and physiologically related photochemical reflectance index variability at the canopy scale over an entire growing season. Plant Cell Environ. 38, 1578–1590.

Houborg, R., McCabe, M., 2018a. Daily retrieval of NDVI and LAI at 3 m resolution via the fusion of CubeSat, Landsat, and MODIS data. Remote Sens. 10, 890.
Houborg, R., McCabe, M.F., 2018b. A Cubesat enabled Spatio-Temporal Enhancement Method (CESTEM) utilizing Planet, Landsat and MODIS data. Remote Sens. Environ. 209, 211–226.
Houborg, R., Cescatti, A., Migliavacca, M., Kustas, W.P., 2013. Satellite retrievals of leaf chlorophyll and photosynthetic capacity for improved modeling of GPP. Agric. For. Meteorol. 177, 10–23.
Houghton, R.A., Hobbie, J.E., Melillo, J.M., Moore, B., Peterson, B.J., Shaver, G.R., Woodwell, G.M., 1983. Changes in the carbon content of terrestrial biota and soils between 1860 and 1980: a net release of CO_2 to the atmosphere. Ecol. Monogr. 53, 236–262.
Huete, A., Didan, K., Miura, T., Rodriguez, E.P., Gao, X., Ferreira, L.G., 2002. Overview of the radiometric and biophysical performance of the MODIS vegetation indices. Remote Sens. Environ. 83, 195–213.
Huete, A.R., Didan, K., Shimabukuro, Y.E., Ratana, P., Saleska, S.R., Hutyra, L.R., Yang, W.Z., Nemani, R.R., Myneni, R., 2006. Amazon rainforests green-up with sunlight in dry season. Geophys. Res. Lett. 33. https://doi.org/10.1029/2005GL025583.
Huete, A.R., Restrepo-Coupe, N., Ratana, P., Didan, K., Saleska, S.R., Ichii, K., Panuthai, S., Gamo, M., 2008. Multiple site tower flux and remote sensing comparisons of tropical forest dynamics in Monsoon Asia. Agric. For. Meteorol. 148, 748–760.
Imhoff, M.L., Bounoua, L., Ricketts, T., Loucks, C., Harriss, R., Lawrence, W.T., 2004. Global patterns in human consumption of net primary production. Nature 429, 870.
Inoue, E., Tani, N., Imai, K., Isobe, S., 1958. The aerodynamic measurement of photosynthesis over the wheat field. J. Agric. Meteorol. 13, 121–125.
Ito, A., 2011. A historical meta-analysis of global terrestrial net primary productivity: are estimates converging? Glob. Chang. Biol. 17, 3161–3175.
Jacquemoud, S., Ustin, S.L., Verdebout, J., Schmuck, G., Andreoli, G., Hosgood, B., 1996. Estimating leaf biochemistry using the PROSPECT leaf optical properties model. Remote Sens. Environ. 56, 194–202.
Jarvis, P.G., 1976. The interpretation of the variations in leaf water potential and stomatal conductance found in canopies in the field. Philos. Trans. R. Soc. Lond. Ser. B Biol. Sci. 273, 593–610.
Jarvis, P.G., 1995. Scaling processes and problems. Plant Cell Environ. 18, 1079–1089.
Jarvis, P.G., McNaughton, K.G., 1986. Stornatal control of transpiration: scaling up from leaf to region. Adv. Ecol. Res. 15, 1–49.
Jiang, C., Ryu, Y., 2016. Multi-scale evaluation of global gross primary productivity and evapotranspiration products derived from Breathing Earth System Simulator (BESS). Remote Sens. Environ. 186, 528–547.
Jiang, C., Ryu, Y., Fang, H., Myneni, R., Claverie, M., Zhu, Z., 2017. Inconsistencies of interannual variability and trends in long-term satellite leaf area index products. Glob. Chang. Biol. 23, 4133–4146.
Joiner, J., Yoshida, Y., Vasilkov, A.P., Yoshida, Y., Corp, L.A., Middleton, E.M., 2011. First observations of global and seasonal terrestrial chlorophyll fluorescence from space. Biogeosciences 8, 637–651.
Joiner, J., Guanter, L., Lindstrot, R., Voigt, M., Vasilkov, A.P., Middleton, E.M., Huemmrich, K.F., Yoshida, Y., Frankenberg, C., 2013. Global monitoring of terrestrial chlorophyll fluorescence from moderate-spectral-resolution near-infrared satellite measurements: methodology, simulations, and application to GOME-2. Atmos. Meas. Tech. 6, 2803–2823.
Joiner, J., Yoshida, Y., Vasilkov, A.P., Schaefer, K., Jung, M., Guanter, L., Zhang, Y., Garrity, S., Middleton, E.M., Huemmrich, K.F., Gu, L., Belelli Marchesini, L., 2014. The seasonal cycle of satellite chlorophyll fluorescence observations and its relationship to vegetation phenology and ecosystem atmosphere carbon exchange. Remote Sens. Environ. 152, 375–391.
Joiner, J., Yoshida, Y., Guanter, L., Middleton, E.M., 2016. New methods for the retrieval of chlorophyll red fluorescence from hyperspectral satellite instruments: simulations and application to GOME-2 and SCIAMACHY. Atmos. Meas. Tech. 9, 3939–3967.
Jordan, C.F., 1969. Derivation of leaf-area index from quality of light on forest floor. Ecology 50, 663–666.
Jung, M., Reichstein, M., Bondeau, A., 2009. Towards global empirical upscaling of FLUXNET eddy covariance observations: validation of a model tree ensemble approach using a biosphere model. Biogeosciences 6, 2001–2013.
Jung, M., Reichstein, M., Ciais, P., Seneviratne, S.I., Sheffield, J., Goulden, M.L., Bonan, G., Cescatti, A., Chen, J., de Jeu, R., Dolman, A.J., Eugster, W., Gerten, D., Gianelle, D., Gobron, N., Heinke, J., Kimball, J., Law, B.E., Montagnani, L., Mu, Q., Mueller, B., Oleson, K., Papale, D., Richardson, A.D., Roupsard, O., Running, S., Tomelleri, E., Viovy, N., Weber, U., Williams, C., Wood, E., Zaehle, S., Zhang, K., 2010. Recent decline in the global land evapotranspiration trend due to limited moisture supply. Nature 467, 951–954.
Jung, M., Reichstein, M., Margolis, H.A., Cescatti, A., Richardson, A.D., Arain, M.A., Arneth, A., Bernhofer, C., Bonal, D., Chen, J.Q., Gianelle, D., Gobron, N., Kiely, G., Kutsch, W., Lasslop, G., Law, B.E., Lindroth, A., Merbold, L., Montagnani, L., Moors, E.J., Papale, D., Sottocornola, M., Vaccari, F., Williams, C., 2011. Global patterns of land-atmosphere fluxes of carbon dioxide, latent heat, and sensible heat derived from eddy covariance, satellite, and meteorological observations. J. Geophys. Res. Biogeosci. 116. https://doi.org/10.1029/2010jg001566.
Jung, M., Reichstein, M., Schwalm, C.R., Huntingford, C., Sitch, S., Ahlström, A., Arneth, A., Camps-Valls, G., Ciais, P., Friedlingstein, P., Gans, F., Ichii, K., Jain, A.K., Kato, E., Papale, D., Poulter, B., Raduly, B., Rödenbeck, C., Tramontana, G., Viovy, N., Wang, Y.-P., Weber, U., Zaehle, S., Zeng, N., 2017. Compensatory water effects link yearly global land CO_2 sink changes to temperature. Nature 541, 516–520.
Jupp, D.L.B., Strahler, A.H., 1991. A hotspot model for leaf canopies. Remote Sens. Environ. 38, 193–210.
Justice, C.O., Townshend, J.R.G., Holben, B.N., Tucker, C.J., 1985. Analysis of the phenology of global vegetation using meteorological satellite data. Int. J. Remote Sens. 6, 1271–1318.
Justice, C.O., Vermote, E., Townshend, J.R.G., Defries, R., Roy, D.P., Hall, D.K., Salomonson, V.V., Privette, J.L., Riggs, G., Strahler, A., Lucht, W., Myneni, R.B., Knyazikhin, Y., Running, S.W., Nemani, R.R., Wan, Z.M., Huete, A.R., van Leeuwen, W., Wolfe, R.E., Giglio, L., Muller, J.P., Lewis, P., Barnsley, M.J., 1998. The Moderate Resolution Imaging Spectroradiometer (MODIS): land remote sensing for global change research. IEEE Trans. Geosci. Remote Sens. 36, 1228–1249.
Kalnay, E., Kanamitsu, M., Kistler, R., Collins, W., Deaven, D., Gandin, L., Iredell, M., Saha, S., White, G., Woollen, J., Zhu, Y., Chelliah, M., Ebisuzaki, W., Higgins, W., Janowiak, J., Mo, K.C., Ropelewski, C., Wang, J., Leetmaa, A., Reynolds, R., Jenne, R., Joseph, D., 1996. The NCEP/NCAR 40-year reanalysis project. Bull. Am. Meteorol. Soc. 77, 437–471.
Kattge, J., Knorr, W., Raddatz, T., Wirth, C., 2009. Quantifying photosynthetic capacity and its relationship to leaf nitrogen content for global-scale terrestrial biosphere models. Glob. Chang. Biol. 15, 976–991.
Kattge, J., Diaz, S., Lavorel, S., Prentice, C., Leadley, P., Bonisch, G., Garnier, E., Westoby, M., Reich, P.B., Wright, I.J., Cornelissen, J.H.C., Violle, C., Harrison, S.P., van Bodegom, P.M., Reichstein, M., Enquist, B.J., Soudzilovskaia, N.A., Ackerly, D.D., Anand, M., Atkin, O., Bahn, M., Baker, T.R., Baldocchi, D., Bekker, R., Blanco, C.C., Blonder, B., Bond, W.J., Bradstock, R., Bunker, D.E., Casanoves, F., Cavender-Bares, J., Chambers, J.Q., Chapin, F.S., Chave, J., Coomes, D., Cornwell, W.K., Craine, J.M., Dobrin, B.H., Duarte, L., Durka, W., Elser, J., Esser, G., Estiarte, M., Fagan, W.F., Fang, J., Fernandez-Mendez, F., Fidelis, A., Finegan, B., Flores, O., Ford, H., Frank, D., Freschet, G.T., Fyllas, N.M., Gallagher, R.V., Green, W.A., Gutierrez, A.G., Hickler, T., Higgins, S.I., Hodgson, J.G., Jalili, A., Jansen, S., Joly, C.A., Kerkhoff, A.J., Kirkup, D., Kitajima, K., Kleyer, M., Klotz, S., Knops, J.M.H., Kramer, K., Kuhn, I., Kurokawa, H., Laughlin, D., Lee, T.D., Leishman, M., Lens, F., Lenz, T., Lewis, S.L., Lloyd, J., Llusia, J., Louault, F., Ma, S., Mahecha, M.D., Manning, P., Massad, T., Medlyn, B.E., Messier, J., Moles, A.T., Muller, S.C., Nadrowski, K., Naeem, S., Niinemets, U., Nollert, S., Nuske, A., Ogaya, R., Oleksyn, J., Onipchenko, V.G., Onoda, Y., Ordonez, J., Overbeck, G., Ozinga, W.A., Patino, S., Paula, S., Pausas, J.G., Penuelas, J., Phillips, O.L., Pillar, V., Poorter, H., Poorter, L., Poschlod, P., Prinzing, A., Proulx, R., Rammig, A., Reinsch, S., Reu, B., Sack, L., Salgado-Negre, B., Sardans, J., Shiodera, S., Shipley, B., Siefert, A., Sosinski, E., Soussana, J.F., Swaine, E., Swenson, N., Thompson, K., Thornton, P., Waldram, M., Weiher, E., White, M., White, S., Wright, S.J., Yguel, B., Zaehle, S., Zanne, A.E., Wirth, C., 2011. TRY - a global database of plant traits. Glob. Chang. Biol. 17, 2905–2935.
Kaufman, Y.J., Tanre, D., Remer, L.A., Vermote, E.F., Chu, A., Holben, B.N., 1997. Operational remote sensing of tropospheric aerosol over land from EOS moderate resolution imaging spectroradiometer. J. Geophys. Res.-Atmos. 102, 17051–17067.
Kautsky, H., 1931. Energie-Umwandlungen an Grenzflächen, IV. Mitteil.: H. Kautsky und A. Hirsch: Wechselwirkung zwischen angeregten Farbstoff-Molekülen und Sauerstoff. Berichte der deutschen chemischen Gesellschaft (A and B Series). 64. pp. 2677–2683.
Keeling, C.D., 1960. The concentration and isotopic abundances of carbon dioxide in the atmosphere. Tellus 12, 200–203.
Keeling, C.D., Chin, J.F.S., Whorf, T.P., 1996. Increased activity of northern vegetation inferred from atmospheric CO_2 measurements. Nature 382, 146–149.
Keenan, T.F., Prentice, I.C., Canadell, J.G., Williams, C.A., Wang, H., Raupach, M., Collatz, G.J., 2016. Recent pause in the growth rate of atmospheric CO_2 due to enhanced terrestrial carbon uptake. Nat. Commun. 7, 13428.
Kerr, Y.H., Waldteufel, P., Wigneron, J., Delwart, S., Cabot, F., Boutin, J., Escorihuela, M., Font, J., Reul, N., Gruhier, C., Juglea, S.E., Drinkwater, M.R., Hahne, A., Martin-Neira, M., Mecklenburg, S., 2010. The SMOS mission: new tool for monitoring key elements ofthe global water cycle. Proc. IEEE 98, 666–687.
Knohl, A., Baldocchi, D.D., 2008. Effects of diffuse radiation on canopy gas exchange processes in a forest ecosystem. J. Geophys. Res. Biogeosci. 113. https://doi.org/10.1029/2007JG000663.
Knyazikhin, Y., Martonchik, J.V., Myneni, R.B., Diner, D.J., Running, S.W., 1998. Synergistic algorithm for estimating vegetation canopy leaf area index and fraction of absorbed photosynthetically active radiation from MODIS and MISR data. J. Geophys. Res.-Atmos. 103, 32257–32275.
Knyazikhin, Y., Lewis, P., Disney, M.I., Stenberg, P., Mõttus, M., Rautiainen, M., Kaufmann, R.K., Marshak, A., Schull, M.A., Latorre Carmona, P., Vanderbilt, V., Davis, A.B., Baret, F., Jacquemoud, S., Lyapustin, A., Yang, Y., Myneni, R.B., 2013a. Reply to Townsend et al.: decoupling contributions from canopy structure and leaf optics is critical for remote sensing leaf biochemistry. Proc. Natl. Acad. Sci. 110, E1075.
Knyazikhin, Y., Schull, M.A., Stenberg, P., Mottus, M., Rautiainen, M., Yang, Y., Marshak, A., Carmona, P.L., Kaufmann, R.K., Lewis, P., Disney, M.I., Vanderbilt, V., Davis, A.B., Baret, F., Jacquemoud, S., Lyapustin, A., Myneni, R.B., 2013b. Hyperspectral remote sensing of foliar nitrogen content. Proc. Natl. Acad. Sci. U. S. A. 110, E185–E192.
Köhler, P., Frankenberg, C., Magney, T.S., Guanter, L., Joiner, J., Landgraf, J., 2018. Global retrievals of solar-induced chlorophyll fluorescence with TROPOMI: first results and intersensor comparison to OCO-2. Geophys. Res. Lett. 45, 10456–10463.
Kokaly, R.F., 2001. Investigating a physical basis for spectroscopic estimates of leaf nitrogen concentration. Remote Sens. Environ. 75, 153–161.
Kondo, M., Ichii, K., Takagi, H., Sasakawa, M., 2015. Comparison of the data-driven top-down and bottom-up global terrestrial CO_2 exchanges: GOSAT CO_2 inversion and empirical eddy flux upscaling. J. Geophys. Res. Biogeosci. 120, 1226–1245.
Kortschak, H.P., Hartt, C.E., Burr, G.O., 1965. Carbon dioxide fixation in sugarcane leaves. Plant Physiol. 40, 209–213.
Krinov, E.L., 1953. Spectral reflectance properties of natural formations. In: Technical Translation (National Research Council of Canada); no. NRC-TT-439. National Research Council of Canada.
Kucharik, C.J., Norman, J.M., Gower, S.T., 1999. Characterization of radiation regimes in nonrandom forest canopies: theory, measurements, and a simplified modeling

approach. Tree Physiol. 19, 695–706.
Kuze, A., Suto, H., Nakajima, M., Hamazaki, T., 2009. Thermal and near infrared sensor for carbon observation Fourier-transform spectrometer on the Greenhouse Gases Observing Satellite for greenhouse gases monitoring. Appl. Opt. 48, 6716–6733.
Laing, W.A., Ogren, W.L., Hageman, R.H., 1974. Regulation of soybean net photosynthetic CO_2 fixation by the interaction of CO_2, O_2, and ribulose 1,5-diphosphate carboxylase. Plant Physiol. 54, 678–685.
Laisk, A., 1970. A model of leaf photosynthesis and photorespiration. In: Malek, I. (Ed.), Prediction and Measurement of Photosynthetic Productivity. Proceeding IBP/PP Technical Meeting, Trebon, Czech. Centre for Agricultural Publishing and Documentation, Wageningen, The Netherlands, pp. 295–306.
Laisk, A., Oja, V.M., 1974. Photosynthesis of leaves subjected to brief impulses of CO_2. Soviet J. Plant Physiol. 21, 928–935.
Larcher, W., 1960. Transpiration and photosynthesis of detached leaves and shoots of *Quercus pubescens* and *Q. ilex* during desiccation under standard conditions. Bull. Res. Counc. Isr. 3 (4), 213–224.
Legg, B.J., 1985. Exchange of carbon dioxide between vegetation and the atmosphere. Plant Cell Environ. 8, 409–416.
Lemon, E.R., 1960. Photosynthesis under field conditions. II. An aerodynamic method for determining the turbulent carbon dioxide exchange between the atmosphere and a corn field1. Agron. J. 52, 697–703.
Lemon, E., Stewart, D.W., Shawcroft, R.W., 1971. The sun's work in a cornfield. Science 174, 371–378.
Leuning, R., 1995. A critical-appraisal of a combined stomatal-photosynthesis model for C-3 plants. Plant Cell Environ. 18, 339–355.
Leuning, R., Kelliher, F.M., Depury, D.G.G., Schulze, E.D., 1995. Leaf nitrogen, photosynthesis, conductance and transpiration - scaling from leaves to canopies. Plant Cell Environ. 18, 1183–1200.
Li, X., Xiao, J., He, B., Altaf Arain, M., Beringer, J., Desai, A.R., Emmel, C., Hollinger, D.Y., Krasnova, A., Mammarella, I., Noe, S.M., Ortiz, P.S., Rey-Sanchez, A.C., Rocha, A.V., Varlagin, A., 2018. Solar-induced chlorophyll fluorescence is strongly correlated with terrestrial photosynthesis for a wide variety of biomes: first global analysis based on OCO-2 and flux tower observations. Glob. Chang. Biol. 24, 3990–4008.
Lieth, H., 1963. The role of vegetation in the carbon dioxide content of the atmosphere. J. Geophys. Res. 68, 3887–3898.
Lieth, H., 1973. Primary production: terrestrial ecosystems. Hum. Ecol. 1, 303–332.
Liu, Y., Liu, R., Chen, J.M., 2012. Retrospective retrieval of long-term consistent global leaf area index (1981–2011) from combined AVHRR and MODIS data. J. Geophys. Res. Biogeosci. 117. https://doi.org/10.1029/2012JG002084.
Liu, X., Liu, L., Hu, J., Du, S., 2017. Modeling the footprint and equivalent radiance transfer path length for tower-based hemispherical observations of chlorophyll fluorescence. Sensors 17, 1131.
Lüdeke, M.K.B., Badeck, F.W., Otto, R.D., Häger, C., Dönges, S., Kindermann, J., Würth, G., Lang, T., Jäkel, U., Klaudius, A., Ramge, P., Habermehl, S., Kohlmaier, G.H., 1994. The Frankfurt Biosphere model: a global process-oriented model of seasonal and long-term CO_2 exchange between terrestrial ecosystems and the atmosphere. I. Model description and illustrative results for cold deciduous and boreal forests. Clim. Res. 4, 143–166.
Luo, X., Keenan, T.F., Fisher, J.B., Jiménez-Muñoz, J.-C., Chen, J.M., Jiang, C., Ju, W., Perakalapudi, N.-V., Ryu, Y., Tadić, J.M., 2018. The impact of the 2015/2016 El Niño on global photosynthesis using satellite remote sensing. Philos. Trans. R. Soc., B 373.
MacDonald, R.B., Hall, F.G., 1980. Global crop forecasting. Science 208, 670–679.
Marshak, A., Herman, J., Szabo, A., Blank, K., Carn, S., Cede, A., Geogdzhayev, I., Huang, D., Huang, L.-K., Knyazikhin, Y., Kowalewski, M., Krotkov, N., Lyapustin, A., McPeters, R., Meyer, K.G., Torres, O., Yang, Y., 2018. Earth observations from DSCOVR EPIC instrument. Bull. Am. Meteorol. Soc. 99, 1829–1850.
Marshall, B., Biscoe, P.V., 1980. A model for C3 leaves describing the dependence of net photosynthesis on irradiance. J. Exp. Bot. 31, 29–39.
Martin, S.T., Andreae, M.O., Artaxo, P., Baumgardner, D., Chen, Q., Goldstein, A.H., Guenther, A., Heald, C.L., Mayol-Bracero, O.L., McMurry, P.H., Pauliquevis, T., Pöschl, U., Prather, K.A., Roberts, G.C., Saleska, S.R., Silva Dias, M.A., Spracklen, D.V., Swietlicki, E., Trebs, I., 2010. Sources and properties of Amazonian aerosol particles. Rev. Geophys. 48. https://doi.org/10.1029/2008RG000280.
Maxwell, K., Johnson, G.N., 2000. Chlorophyll fluorescence—a practical guide. J. Exp. Bot. 51, 659–668.
McAlister, E.D., Myers, J., 1940. Time course of photosynthesis and fluorescence. Science 92, 241–243.
McColl, K.A., Alemohammad, S.H., Akbar, R., Konings, A.G., Yueh, S., Entekhabi, D., 2017. The global distribution and dynamics of surface soil moisture. Nat. Geosci. 10, 100.
McNaughton, K.G., Jarvis, P.G., 1991. Effects of spatial scale on stomatal control of transpiration. Agric. For. Meteorol. 54, 279–302.
Medlyn, B.E., 2004. A MAESTRO retrospective. In: Mencuccini, M., Grace, J.G., Moncrieff, J., McNaughton, K. (Eds.), Forests at the Land-Atmosphere Interface. CAB International, pp. 105–121.
Medlyn, B.E., 2011. Comment on “drought-induced reduction in global terrestrial net primary production from 2000 through 2009”. Science 333, 1093.
Medlyn, B.E., Robinson, A.P., Clement, R., McMurtrie, R.E., 2005. On the validation of models of forest CO_2 exchange using eddy covariance data: some perils and pitfalls. Tree Physiol. 25, 839–857.
Melillo, J.M., McGuire, A.D., Kicklighter, D.W., Moore, B., Vorosmarty, C.J., Schloss, A.L., 1993. Global climate change and terrestrial net primary production. Nature 363, 234.
Mercado, L.M., Bellouin, N., Sitch, S., Boucher, O., Huntingford, C., Wild, M., Cox, P.M., 2009. Impact of changes in diffuse radiation on the global land carbon sink. Nature 458, 1014–1017.
Meroni, M., Rossini, M., Guanter, L., Alonso, L., Rascher, U., Colombo, R., Moreno, J., 2009. Remote sensing of solar-induced chlorophyll fluorescence: review of methods and applications. Remote Sens. Environ. 113, 2037–2051.
Migliavacca, M., Perez-Priego, O., Rossini, M., El-Madany, T.S., Moreno, G., van der Tol, C., Rascher, U., Berninger, A., Bessenbacher, V., Burkart, A., Carrara, A., Fava, F., Guan, J.-H., Hammer, T.W., Henkel, K., Juarez-Alcalde, E., Julitta, T., Kolle, O., Martín, M.P., Musavi, T., Pacheco-Labrador, J., Pérez-Burgueño, A., Wutzler, T., Zaehle, S., Reichstein, M., 2017. Plant functional traits and canopy structure control the relationship between photosynthetic CO_2 uptake and far-red sun-induced fluorescence in a Mediterranean grassland under different nutrient availability. New Phytol. 214, 1078–1091.
Monsi, M., Saeki, T., 1953. Über den lichtfaktor in den pflanzengesellschaften und seine bedeutung für die stoffproduktion. Jpn. J. Bot. 14, 22–52.
Monsi, M., Saeki, T., 2005. On the factor light in plant communities and its importance for matter production. Ann. Bot. 95, 549–567.
Monteith, J.L., 1965. Light distribution and photosynthesis in field crops. Ann. Bot. 29, 17–37.
Monteith, J.L., 1972. Solar radiation and productivity in tropical ecosystems. J. Appl. Ecol. 9, 747–766.
Monteith, J.L., 1977. Climate and efficiency of crop production in Britain. Philos. Trans. R. Soc. Lond. Ser. B Biol. Sci. 281, 277–294.
Moreno-Martínez, Á., Camps-Valls, G., Kattge, J., Robinson, N., Reichstein, M., van Bodegom, P., Kramer, K., Cornelissen, J.H.C., Reich, P., Bahn, M., Niinemets, Ü., Peñuelas, J., Craine, J.M., Cerabolini, B.E.L., Minden, V., Laughlin, D.C., Sack, L., Allred, B., Baraloto, C., Byun, C., Soudzilovskaia, N.A., Running, S.W., 2018. A methodology to derive global maps of leaf traits using remote sensing and climate data. Remote Sens. Environ. 218, 69–88.
Morton, D.C., Nagol, J., Carabajal, C.C., Rosette, J., Palace, M., Cook, B.D., Vermote, E.F., Harding, D.J., North, P.R.J., 2014. Amazon forests maintain consistent canopy structure and greenness during the dry season. Nature 506, 221–224.
Moss, R.A., Loomis, W.E., 1952. Absorption spectra of leaves. I. The visible spectrum. Plant Physiol. 27, 370–391.
Moss, D.N., Musgrave, R.B., Lemon, E.R., 1961. Photosynthesis under field conditions. III. Some effects of light, carbon dioxide, temperature, and soil moisture on photosynthesis, respiration, and transpiration of corn1. Crop Sci. 1, 83–87.
Moya, I., Camenen, L., Evain, S., Goulas, Y., Cerovic, Z.G., Latouche, G., Flexas, J., Ounis, A., 2004. A new instrument for passive remote sensing: 1. Measurements of sunlight-induced chlorophyll fluorescence. Remote Sens. Environ. 91, 186–197.
Muraoka, H., Koizumi, H., 2005. Photosynthetic and structural characteristics of canopy and shrub trees in a cool-temperate deciduous broadleaved forest: implication to the ecosystem carbon gain. Agric. For. Meteorol. 134, 39–59.
Musgrave, R.B., Moss, D.N., 1961. Photosynthesis under field conditions. I. A portable, closed system for determining the rate of photosynthesis and respiration in corn. Crop Sci. 1, 37–41.
Myneni, R.B., Ross, J., Asrar, G., 1989. A review on the theory of photon transport in leaf canopies. Agric. For. Meteorol. 45, 1–153.
Myneni, R.B., Keeling, C.D., Tucker, C.J., Asrar, G., Nemani, R.R., 1997. Increased plant growth in the northern high latitudes from 1981 to 1991. Nature 386, 698–702.
Myneni, R.B., Hoffman, S., Knyazikhin, Y., Privette, J.L., Glassy, J., Tian, Y., Wang, Y., Song, X., Zhang, Y., Smith, G.R., 2002. Global products of vegetation leaf area and fraction absorbed PAR from year one of MODIS data. Remote Sens. Environ. 83, 214–231.
Myneni, R.B., Yang, W.Z., Nemani, R.R., Huete, A.R., Dickinson, R.E., Knyazikhin, Y., Didan, K., Fu, R., Juarez, R.I.N., Saatchi, S.S., Hashimoto, H., Ichii, K., Shabanov, N.V., Tan, B., Ratana, P., Privette, J.L., Morisette, J.T., Vermote, E.F., Roy, D.P., Wolfe, R.E., Friedl, M.A., Running, S.W., Votava, P., El-Saleous, N., Devadiga, S., Su, Y., Salomonson, V.V., 2007. Large seasonal swings in leaf area of Amazon rainforests. Proc. Natl. Acad. Sci. U. S. A. 104, 4820–4823.
Nakaji, T., Kosugi, Y., Takanashi, S., Niiyama, K., Noguchi, S., Tani, M., Oguma, H., Nik, A.R., Kassim, A.R., 2014. Estimation of light-use efficiency through a combinational use of the photochemical reflectance index and vapor pressure deficit in an evergreen tropical rainforest at Pasoh, Peninsular Malaysia. Remote Sens. Environ. 150, 82–92.
National Academies of Sciences, E., & Medicine, 2018. Thriving on Our Changing Planet: A Decadal Strategy for Earth Observation From Space. The National Academies Press, Washington, DC.
Nemani, R.R., Running, S.W., 1989. Estimation of regional surface resistance to evapotranspiration. J. Appl. Meteorol. 28, 276–284.
Nemani, R., Votava, P., Michaelis, A., Melton, F., Milesi, C., 2011. Collaborative supercomputing for global change science. EOS Trans. Am. Geophys. Union 92, 109–110.
Nichiporovich, A.A., 1961. On properties of plants as an optical system. Soviet Plant Physiol. 8, 536–546.
Nilson, T., 1971. Theoretical analysis of frequency of gaps in plant stands. Agric. Meteorol. 8, 25–38.
Niyogi, D., Chang, H.I., Saxena, V.K., Holt, T., Alapaty, K., Booker, F., Chen, F., Davis, K.J., Holben, B., Matsui, T., Meyers, T., Oechel, W.C., Pielke, R.A., Wells, R., Wilson, K., Xue, Y.K., 2004. Direct observations of the effects of aerosol loading on net ecosystem CO_2 exchanges over different landscapes. Geophys. Res. Lett. 31. https://doi.org/10.1029/2004GL020915.
Norman, J.M., 1979. Modeling the complete crop canopy. In: Barfield, B.J., Gerber, J.F. (Eds.), Modification of the Aerial Environment of Crops. American Society of Agricultural Engineers, pp. 249–280.
Ollinger, S.V., Richardson, A.D., Martin, M.E., Hollinger, D.Y., Frolking, S.E., Reich, P.B., Plourde, L.C., Katul, G.G., Munger, J.W., Oren, R., Smith, M.L., Paw, U., K., T., Bolstad, P.V., Cook, B.D., Day, M.C., Martin, T.A., Monson, R.K., Schmid, H.P., 2008. Canopy nitrogen, carbon assimilation, and albedo in temperate and boreal forests: functional relations and potential climate feedbacks. Proc. Natl. Acad. Sci. U. S. A. 105, 19336–19341.

Olson, J.S., Watts, J.A., Allison, L.J., 1983. Carbon in Live Vegetation of Major World Ecosystems (ORNL-5862). Environmental Sciences Division, Oak Ridge National Laboratory, Oak Ridge, Tennessee.
Olson, J.S., Watts, J.A., Allison, L.J., 1985. Major World Ecosystem Complexes Ranked by Carbon in Live Vegetation: A Database. NDP-017. Carbon Dioxide Information Center, Oak Ridge National Laboratory, Oak Ridge, Tennessee.
Oreskes, N., Shrader-Frechette, K., Belitz, K., 1994. Verification, validation, and confirmation of numerical models in the earth sciences. Science 263, 641–646.
Osmond, C.B., Björkman, O., Anderson, D.J., 1980. Physiological Processes in Plant Ecology: Towards a Synthesis With Atriplex. Springer-Verlag, Berlin.
Papale, D., Valentini, R., 2003. A new assessment of European forests carbon exchanges by eddy fluxes and artificial neural network spatialization. Glob. Chang. Biol. 9, 525–535.
Papale, D., Black, T.A., Carvalhais, N., Cescatti, A., Chen, J., Jung, M., Kiely, G., Lasslop, G., Mahecha, M.D., Margolis, H., Merbold, L., Montagnani, L., Moors, E., Olesen, J.E., Reichstein, M., Tramontana, G., van Gorsel, E., Wohlfahrt, G., Ráduly, B., 2015. Effect of spatial sampling from European flux towers for estimating carbon and water fluxes with artificial neural networks. J. Geophys. Res. Biogeosci. 120, 1941–1957.
Paul-Limoges, E., Damm, A., Hueni, A., Liebisch, F., Eugster, W., Schaepman, M.E., Buchmann, N., 2018. Effect of environmental conditions on sun-induced fluorescence in a mixed forest and a cropland. Remote Sens. Environ. 219, 310–323.
Penuelas, J., Filella, I., Gamon, J.A., 1995. Assessment of photosynthetic radiation-use efficiency with spectral reflectance. New Phytol. 131, 291–296.
Pinker, R.T., Laszlo, I., 1992. Modeling surface solar irradiance for satellite applications on a global scale. J. Appl. Meteorol. 31, 194–211.
Pisek, J., Sonnentag, O., Richardson, A.D., Mõttus, M., 2013. Is the spherical leaf inclination angle distribution a valid assumption for temperate and boreal broadleaf tree species? Agric. For. Meteorol. 169, 186–194.
Porcar-Castell, A., Tyystjärvi, E., Atherton, J., van der Tol, C., Flexas, J., Pfündel, E.E., Moreno, J., Frankenberg, C., Berry, J.A., 2014. Linking chlorophyll a fluorescence to photosynthesis for remote sensing applications: mechanisms and challenges. J. Exp. Bot. 65, 4065–4095.
Potter, C.S., Randerson, J.T., Field, C.B., Matson, P.A., Vitousek, P.M., Mooney, H.A., Klooster, S.A., 1993. Terrestrial ecosystem production - a process model-based on global satellite and surface data. Glob. Biogeochem. Cycles 7, 811–841.
Prentice, I.C., Cramer, W., Harrison, S.P., Leemans, R., Monserud, R.A., Solomon, A.M., 1992. A global biome model based on plant physiology and dominance, soil properties and climate. J. Biogeogr. 19, 117–134.
Prince, S.D., Goward, S.N., 1995. Global primary production: a remote sensing approach. J. Biogeogr. 22, 815–835.
Rabinowitch, E.I., 1951. Photosynthesis and Related Processes. Wiley Inter Science, New York.
Randall, D.A., Dazlich, D.A., Zhang, C., Denning, A.S., Sellers, P.J., Tucker, C.J., Bounoua, L., Los, S.O., Justice, C.O., Fung, I., 1996. A revised land surface parameterization (SiB2) for GCMs. 3. The greening of the Colorado State University general circulation model. J. Clim. 9, 738–763.
Rascher, U., Alonso, L., Burkart, A., Cilia, C., Cogliati, S., Colombo, R., Damm, A., Drusch, M., Guanter, L., Hanus, J., Hyvärinen, T., Julitta, T., Jussila, J., Kataja, K., Kokkalis, P., Kraft, S., Kraska, T., Matveeva, M., Moreno, J., Muller, O., Panigada, C., Pikl, M., Pinto, F., Prey, L., Pude, R., Rossini, M., Schickling, A., Schurr, U., Schüttemeyer, D., Verrelst, J., Zemek, F., 2015. Sun-induced fluorescence – a new probe of photosynthesis: first maps from the imaging spectrometer HyPlant. Glob. Chang. Biol. 21, 4673–4684.
Raschke, K., 1960. Heat transfer between the plant and the environment. Annu. Rev. Plant Physiol. 11, 111–126.
Raupach, M.R., Finnigan, J.J., 1988. 'Single-layer models of evaporation from plant canopies are incorrect but useful, whereas multilayer models are correct but useless': discuss. Aust. J. Plant Physiol. 15, 705–716.
Reichstein, M., Falge, E., Baldocchi, D., Papale, D., Aubinet, M., Berbigier, P., Bernhofer, C., Buchmann, N., Gilmanov, T., Granier, A., Grunwald, T., Havrankova, K., Ilvesniemi, H., Janous, D., Knohl, A., Laurila, T., Lohila, A., Loustau, D., Matteucci, G., Meyers, T., Miglietta, F., Ourcival, J.M., Pumpanen, J., Rambal, S., Rotenberg, E., Sanz, M., Tenhunen, J., Seufert, G., Vaccari, F., Vesala, T., Yakir, D., Valentini, R., 2005. On the separation of net ecosystem exchange into assimilation and ecosystem respiration: review and improved algorithm. Glob. Chang. Biol. 11, 1424–1439.
Rienecker, M.M., Suarez, M.J., Gelaro, R., Todling, R., Bacmeister, Julio, Liu, E., Bosilovich, M.G., Schubert, S.D., Takacs, L., Kim, G.-K., Bloom, S., Chen, J., Collins, D., Conaty, A., Silva, A.d., Gu, W., Joiner, J., Koster, R.D., Lucchesi, R., Molod, A., Owens, T., Pawson, S., Pegion, P., Redder, C.R., Reichle, R., Robertson, F.R., Ruddick, A.G., Sienkiewicz, M., Woollen, J., 2011. MERRA: NASA's modern-era retrospective analysis for research and applications. J. Clim. 24, 3624–3648.
Rockstrom, J., Steffen, W., Noone, K., Persson, A., Chapin, F.S., Lambin, E.F., Lenton, T.M., Scheffer, M., Folke, C., Schellnhuber, H.J., Nykvist, B., de Wit, C.A., Hughes, T., van der Leeuw, S., Rodhe, H., Sorlin, S., Snyder, P.K., Costanza, R., Svedin, U., Falkenmark, M., Karlberg, L., Corell, R.W., Fabry, V.J., Hansen, J., Walker, B., Liverman, D., Richardson, K., Crutzen, P., Foley, J.A., 2009. A safe operating space for humanity. Nature 461, 472–475.
Roderick, M.L., Farquhar, G.D., Berry, S.L., Noble, I.R., 2001. On the direct effect of clouds and atmospheric particles on the productivity and structure of vegetation. Oecologia 129, 21–30.
Ross, J., 1981. The Radiation Regime and Architecture of Plant Stands. Junk Publishers, The Hague.
Rossini, M., Nedbal, L., Guanter, L., Ač, A., Alonso, L., Burkart, A., Cogliati, S., Colombo, R., Damm, A., Drusch, M., Hanus, J., Janoutova, R., Julitta, T., Kokkalis, P., Moreno, J., Novotny, J., Panigada, C., Pinto, F., Schickling, A., Schüttemeyer, D., Zemek, F., Rascher, U., 2015. Red and far red Sun-induced chlorophyll fluorescence as a measure of plant photosynthesis. Geophys. Res. Lett. 42, 1632–1639.
Rouse, J.W., Haas, R.H., Schell, J.A., Deering, D.W., 1973. Monitoing vegetation systems in the great plains with ERTS. In: Third ERTS Symposium, NASA SP-351. 1. pp. 309–317.
Ruel, J.J., Ayres, M.P., 1999. Jensen's inequality predicts effects of environmental variation. Trends Ecol. Evol. 14, 361–366.
Ruimy, A., Saugier, B., Dedieu, G., 1994. Methodology for the estimation of terrestrial net primary production from remotely sensed data. J. Geophys. Res.-Atmos. 99, 5263–5283.
Ruimy, A., Dedieu, G., Saugier, B., 1996. TURC: a diagnostic model of continental gross primary productivity and net primary productivity. Glob. Biogeochem. Cycles 10, 269–285.
Running, S.W., 1990. Estimating terrestrial primary productivity by combining remote sensing and ecosystem simulation. In: Hobbs, R.J., Mooney, H.A. (Eds.), Remote Sensing of Biosphere Functioning. Springer New York, New York, NY, pp. 65–86.
Running, S.W., 2012. A measurable planetary boundary for the biosphere. Science 337, 1458–1459.
Running, S.W., Nemani, R.R., 1988. Relating seasonal patterns of the AVHRR vegetation index to simulated photosynthesis and transpiration of forests in different climates. Remote Sens. Environ. 24, 347–367.
Running, S.W., Justice, C.O., Salomonson, V., Hall, D., Barker, J., Kaufmann, Y.J., Strahler, A.H., Huete, A.R., Muller, J.P., Vanderbilt, V., Wan, Z.M., Teillet, P., Carneggie, D., 1994. Terrestrial remote sensing science and algorithms planned for EOS/MODIS. Int. J. Remote Sens. 15, 3587–3620.
Running, S.W., Baldocchi, D.D., Turner, D.P., Gower, S.T., Bakwin, P.S., Hibbard, K.A., 1999. A global terrestrial monitoring network integrating tower fluxes, flask sampling, ecosystem modeling and EOS satellite data. Remote Sens. Environ. 70, 108–127.
Running, S.W., Thornton, P.E., Nemani, R.R., Glassy, J.M., 2000. Global terrestrial gross and net primary productivity from the earth observing system. In: Sala, O.E. (Ed.), Methods in Ecosystem Science. Springer.
Running, S.W., Nemani, R.R., Heinsch, F.A., Zhao, M.S., Reeves, M., Hashimoto, H., 2004. A continuous satellite-derived measure of global terrestrial primary production. Bioscience 54, 547–560.
Ryu, Y., Sonnentag, O., Nilson, T., Vargas, R., Kobayashi, H., Wenk, R., Baldocchi, D.D., 2010. How to quantify tree leaf area index in a heterogeneous savanna ecosystem: a multi-instrument and multi-model approach. Agric. For. Meteorol. 150, 63–76.
Ryu, Y., Baldocchi, D.D., Kobayashi, H., van Ingen, C., Li, J., Black, T.A., Beringer, J., van Gorsel, E., Knohl, A., Law, B.E., Roupsard, O., 2011. Integration of MODIS land and atmosphere products with a coupled-process model to estimate gross primary productivity and evapotranspiration from 1 km to global scales. Glob. Biogeochem. Cycles 25 (GB4017). https://doi.org/10.1029/2011GB004053.
Ryu, Y., Baldocchi, D.D., Black, T.A., Detto, M., Law, B.E., Leuning, R., Miyata, A., Reichstein, M., Vargas, R., Ammann, C., Beringer, J., Flanagan, L.B., Gu, L., Hutley, L.B., Kim, J., McCaughey, H., Moors, E.J., Rambal, S., Vesala, T., 2012. On the temporal upscaling of evapotranspiration from instantaneous remote sensing measurements to 8-day mean daily-sums. Agric. For. Meteorol. 152, 212–222.
Ryu, Y., Jiang, C., Kobayashi, H., Detto, M., 2018. MODIS-derived global land products of shortwave radiation and diffuse and total photosynthetically active radiation at 5 km resolution from 2000. Remote Sens. Environ. 204, 812–825.
Saleska, S.R., Didan, K., Huete, A.R., da Rocha, H.R., 2007. Amazon forests green-up during 2005 drought. Science 318, 612.
Samanta, A., Ganguly, S., Hashimoto, H., Devadiga, S., Vermote, E., Knyazikhin, Y., Nemani, R.R., Myneni, R.B., 2010. Amazon forests did not green-up during the 2005 drought. Geophys. Res. Lett. 37. https://doi.org/10.1029/2009GL042154.
Schaefer, K., Schwalm, C.R., Williams, C., Arain, M.A., Barr, A., Chen, J.M., Davis, K.J., Dimitrov, D., Hilton, T.W., Hollinger, D.Y., Humphreys, E., Poulter, B., Raczka, B.M., Richardson, A.D., Sahoo, A., Thornton, P., Vargas, R., Verbeeck, H., Anderson, R., Baker, I., Black, T.A., Bolstad, P., Chen, J., Curtis, P.S., Desai, A.R., Dietze, M., Dragoni, D., Gough, C., Grant, R.F., Gu, L., Jain, A., Kucharik, C., Law, B., Liu, S., Lokipitiya, E., Margolis, H.A., Matamala, R., McCaughey, J.H., Monson, R., Munger, J.W., Oechel, W., Peng, C., Price, D.T., Ricciuto, D., Riley, W.J., Roulet, N., Tian, H., Tonitto, C., Torn, M., Weng, E., Zhou, X., 2012. A model-data comparison of gross primary productivity: results from the North American Carbon Program site synthesis. J. Geophys. Res. Biogeosci. 117. https://doi.org/10.1029/2012JG001960.
Schimel, D., Pavlick, R., Fisher, J.B., Asner, G.P., Saatchi, S., Townsend, P., Miller, C., Frankenberg, C., Hibbard, K., Cox, P., 2015. Observing terrestrial ecosystems and the carbon cycle from space. Glob. Chang. Biol. 21, 1762–1776.
Schroeder, H., 1919. Die jahrliche gesamtproduktion der grunen pflanzendecke der erde. Naturwissenschaften 7, 8–12.
Schulze, E.D., Mooney, H.A., Dunn, E.L., 1967. Wintertime photosynthesis of bristlecone pine (*Pinus aristata*) in the White Mountains of California. Ecology 48, 1044–1047.
Schulze, E.D., Kelliher, F.M., Korner, C., Lloyd, J., Leuning, R., 1994. Relationships among maximum stomatal conductance, ecosystem surface conductance, carbon assimilation rate, and plant nitrogen nutrition - a global ecology scaling exercise. Annu. Rev. Ecol. Syst. 25, 629–660.
Schwandner, F.M., Gunson, M.R., Miller, C.E., Carn, S.A., Eldering, A., Krings, T., Verhulst, K.R., Schimel, D.S., Nguyen, H.M., Crisp, D., O'Dell, C.W., Osterman, G.B., Iraci, L.T., Podolske, J.R., 2017. Spaceborne detection of localized carbon dioxide sources. Science 358.
Sellers, P.J., 1985. Canopy reflectance, photosynthesis and transpiration. Int. J. Remote Sens. 6, 1335–1372.
Sellers, P.J., 1987. Canopy reflectance, photosynthesis, and transpiration, II. The role of biophysics in the linearity of their interdependence. Remote Sens. Environ. 21, 143–183.
Sellers, P., Schimel, D., 1993. Remote sensing of the land biosphere and biogeochemistry

in the EOS era: science priorities, methods and implementation—EOS land biosphere and biogeochemical cycles panels. Glob. Planet. Chang. 7, 279–297.
Sellers, P.J., Mintz, Y., Sud, Y.C., Dalcher, A., 1986. A simple biosphere model (SiB) for use within general-circulation models. J. Atmos. Sci. 43, 505–531.
Sellers, P.J., Hall, F.G., Asrar, G., Strebel, D.E., Murphy, R.E., 1992. An overview of the first international satellite land surface climatology project (ISLSCP) field experiment (FIFE). J. Geophys. Res.-Atmos. 97, 18345–18371.
Sellers, P., Hall, F., Margolis, H., Kelly, B., Baldocchi, D., Hartog, G.d., Cihlar, J., Ryan, M.G., Goodison, B., Crill, P., Ranson, K.J., Lettenmaier, D., Wickland, D.E., 1995. The boreal ecosystem–atmosphere study (BOREAS): an overview and early results from the 1994 field year. Bull. Am. Meteorol. Soc. 76, 1549–1577.
Sellers, P.J., Los, S.O., Tucker, C.J., Justice, C.O., Dazlich, D.A., Collatz, G.J., Randall, D.A., 1996a. A revised land surface parameterization (SiB2) for atmospheric GCMs. 2. The generation of global fields of terrestrial biophysical parameters from satellite data. J. Clim. 9, 706–737.
Sellers, P.J., Randall, D.A., Collatz, G.J., Berry, J.A., Field, C.B., Dazlich, D.A., Zhang, C., Collelo, G.D., Bounoua, L., 1996b. A revised land surface parameterization (SiB2) for atmospheric GCMs. part 1: model formulation. J. Clim. 9, 676–705.
Sellers, P.J., Dickinson, R.E., Randall, D.A., Betts, A.K., Hall, F.G., Berry, J.A., Collatz, G.J., Denning, A.S., Mooney, H.A., Nobre, C.A., Sato, N., Field, C.B., HendersonSellers, A., 1997. Modeling the exchanges of energy, water, and carbon between continents and the atmosphere. Science 275, 502–509.
Sellers, P.J., Schimel, D.S., Moore, B., Liu, J., Eldering, A., 2018. Observing carbon cycle–climate feedbacks from space. Proc. Natl. Acad. Sci. U. S. A. 115, 7860–7868.
Seneviratne, S.I., Donat, M.G., Mueller, B., Alexander, L.V., 2014. No pause in the increase of hot temperature extremes. Nat. Clim. Chang. 4, 161–163.
Serbin, S.P., Dillaway, D.N., Kruger, E.L., Townsend, P.A., 2012. Leaf optical properties reflect variation in photosynthetic metabolism and its sensitivity to temperature. J. Exp. Bot. 63, 489–502.
Serbin, S.P., Singh, A., Desai, A.R., Dubois, S.G., Jablonski, A.D., Kingdon, C.C., Kruger, E.L., Townsend, P.A., 2015. Remotely estimating photosynthetic capacity, and its response to temperature, in vegetation canopies using imaging spectroscopy. Remote Sens. Environ. 167, 78–87.
Shukla, J., Mintz, Y., 1982. Influence of land-surface evapotranspiration on the Earth's climate. Science 215, 1498–1501.
Shull, C.A., 1929. A spectrophotometric study of reflection of light from leaf surfaces. Bot. Gaz. 87, 583–607.
Siegenthaler, U., Sarmiento, J.L., 1993. Atmospheric carbon dioxide and the ocean. Nature 365, 119.
Sims, D.A., Rahman, A.F., Cordova, V.D., El-Masri, B.Z., Baldocchi, D.D., Flanagan, L.B., Goldstein, A.H., Hollinger, D.Y., Misson, L., Monson, R.K., Oechel, W.C., Schmid, H.P., Wofsy, S.C., Xu, L., 2006. On the use of MODIS EVI to assess gross primary productivity of North American ecosystems. J. Geophys. Res. 111. https://doi.org/10.1029/2006JG000162.
Sims, D.A., Rahman, A.F., Cordova, V.D., El-Masri, B.Z., Baldocchi, D.D., Bolstad, P.V., Flanagan, L.B., Goldstein, A.H., Hollinger, D.Y., Misson, L., Monson, R.K., Oechel, W.C., Schmid, H.P., Wofsy, S.C., Xu, L., 2008. A new model of gross primary productivity for North American ecosystems based solely on the enhanced vegetation index and land surface temperature from MODIS. Remote Sens. Environ. 112, 1633–1646.
Sinclair, T.R., Murphy, C.E., Knoerr, K.R., 1976. Development and evaluation of simplified models for simulating canopy photosynthesis and transpiration. J. Appl. Ecol. 13, 813–829.
Singh, A., Serbin, S.P., McNeil, B.E., Kingdon, C.C., Townsend, P.A., 2015. Imaging spectroscopy algorithms for mapping canopy foliar chemical and morphological traits and their uncertainties. Ecol. Appl. 25, 2180–2197.
Skole, D., Tucker, C., 1993. Tropical deforestation and habitat fragmentation in the Amazon: satellite data from 1978 to 1988. Science 260, 1905–1910.
Smith, W.K., Reed, S.C., Cleveland, C.C., Ballantyne, A.P., Anderegg, W.R.L., Wieder, W.R., Liu, Y.Y., Running, S.W., 2016. Large divergence of satellite and Earth system model estimates of global terrestrial CO_2 fertilization. Nat. Clim. Chang. 6, 306–310.
Smith, W.K., Biederman, J.A., Scott, R.L., Moore, D.J.P., He, M., Kimball, J.S., Yan, D., Hudson, A., Barnes, M.L., MacBean, N., Fox, A.M., Litvak, M.E., 2018. Chlorophyll fluorescence better captures seasonal and interannual gross primary productivity dynamics across dryland ecosystems of southwestern north America. Geophys. Res. Lett. 45, 748–757.
Stenberg, P., Mõttus, M., Rautiainen, M., 2016. Photon recollision probability in modelling the radiation regime of canopies — a review. Remote Sens. Environ. 183, 98–108.
Still, C.J., Berry, J.A., Collatz, G.J., DeFries, R.S., 2003. Global distribution of C3 and C4 vegetation: carbon cycle implications. Glob. Biogeochem. Cycles 17 (1). https://doi.org/10.1029/2001GB001807.
Stocker, B.D., Zscheischler, J., Keenan, T.F., Prentice, I.C., Peñuelas, J., Seneviratne, S.I., 2018. Quantifying soil moisture impacts on light use efficiency across biomes. New Phytol. 218, 1430–1449.
Stockli, R., Rutishauser, T., Dragoni, D., O'Keefe, J., Thornton, P.E., Jolly, M., Lu, L., Denning, A.S., 2008. Remote sensing data assimilation for a prognostic phenology model. J. Geophys. Res. Biogeosci. 113. https://doi.org/10.1029/2008JG000781.
Sun, Y., Frankenberg, C., Wood, J.D., Schimel, D.S., Jung, M., Guanter, L., Drewry, D.T., Verma, M., Porcar-Castell, A., Griffis, T.J., Gu, L., Magney, T.S., Köhler, P., Evans, B., Yuen, K., 2017. OCO-2 advances photosynthesis observation from space via solar-induced chlorophyll fluorescence. Science 358.
Tans, P.P., Fung, I.Y., Takahashi, T., 1990. Observational constraints on the global atmospheric CO_2 budget. Science 247, 1431–1438.
Tatem, A.J., Goetz, S.J., Hay, S.I., 2008. Fifty years of Earth-observation satellites: views from space have led to countless advances on the ground in both scientific knowledge and daily life. Am. Sci. 96, 390–398.
Tenhunen, J.D., Yocum, C.S., Gates, D.M., 1976. Development of a photosynthesis model with an emphasis on ecological applications. Oecologia 26, 89–100.
Thomas, M.D., Hill, G.R., 1937. The continuous measurement of photosynthesis, respiration and transpiration of alfalfa and wheat growing under field conditions. Plant Physiol. 12, 285–307.
Townsend, P.A., Serbin, S.P., Kruger, E.L., Gamon, J.A., 2013. Disentangling the contribution of biological and physical properties of leaves and canopies in imaging spectroscopy data. Proc. Natl. Acad. Sci. 110, E1074.
Townshend, J., Justice, C., Li, W., Gurney, C., McManus, J., 1991. Global land cover classification by remote sensing: present capabilities and future possibilities. Remote Sens. Environ. 35, 243–255.
Tramontana, G., Jung, M., Schwalm, C.R., Ichii, K., Camps-Valls, G., Ráduly, B., Reichstein, M., Arain, M.A., Cescatti, A., Kiely, G., Merbold, L., Serrano-Ortiz, P., Sickert, S., Wolf, S., Papale, D., 2016. Predicting carbon dioxide and energy fluxes across global FLUXNET sites with regression algorithms. Biogeosciences 13, 4291–4313.
Tranquillini, W., 1957. Standortsklima, wasserbilanz und CO_2-gaswechsel junger zirben (*Pinus cembra* L.) an der alpinen waldgrenze. Planta 49, 612–661.
Tucker, C.J., 1979. Red and photographic infrared linear combinations for monitoring vegetation. Remote Sens. Environ. 8, 127–150.
Tucker, C.J., Townshend, J.R.G., Goff, T.E., 1985. African land-cover classification using satellite data. Science 227, 369–375.
Tucker, C.J., Fung, I.Y., Keeling, C.D., Gammon, R.H., 1986. Relationship between atmospheric CO_2 variations and a satellite-derived vegetation index. Nature 319, 195–199.
Tucker, C.J., Pinzon, J.E., Brown, M.E., Slayback, D.A., Pak, E.W., Mahoney, R., Vermote, E.F., El Saleous, N., 2005. An extended AVHRR 8-km NDVI dataset compatible with MODIS and SPOT vegetation NDVI data. Int. J. Remote Sens. 26, 4485–4498.
Turner, D.P., Ritts, W.D., Cohen, W.B., Gower, S.T., Zhao, M.S., Running, S.W., Wofsy, S.C., Urbanski, S., Dunn, A.L., Munger, J.W., 2003. Scaling Gross Primary Production (GPP) over boreal and deciduous forest landscapes in support of MODIS GPP product validation. Remote Sens. Environ. 88, 256–270.
Turner, D.P., Ritts, W.D., Cohen, W.B., Gower, S.T., Running, S.W., Zhao, M.S., Costa, M.H., Kirschbaum, A.A., Ham, J.M., Saleska, S.R., Ahl, D.E., 2006. Evaluation of MODIS NPP and GPP products across multiple biomes. Remote Sens. Environ. 102, 282–292.
Uppala, S.M., Kallberg, P.W., Simmons, A.J., Andrae, U., Bechtold, V.D., Fiorino, M., Gibson, J.K., Haseler, J., Hernandez, A., Kelly, G.A., Li, X., Onogi, K., Saarinen, S., Sokka, N., Allan, R.P., Andersson, E., Arpe, K., Balmaseda, M.A., Beljaars, A.C.M., Van De Berg, L., Bidlot, J., Bormann, N., Caires, S., Chevallier, F., Dethof, A., Dragosavac, M., Fisher, M., Fuentes, M., Hagemann, S., Holm, E., Hoskins, B.J., Isaksen, L., Janssen, P., Jenne, R., McNally, A.P., Mahfouf, J.F., Morcrette, J.J., Rayner, N.A., Saunders, R.W., Simon, P., Sterl, A., Trenberth, K.E., Untch, A., Vasiljevic, D., Viterbo, P., Woollen, J., 2005. The ERA-40 re-analysis. Q. J. R. Meteorol. Soc. 131, 2961–3012.
Valentini, R., Matteucci, G., Dolman, A.J., Schulze, E.D., Rebmann, C., Moors, E.J., Granier, A., Gross, P., Jensen, N.O., Pilegaard, K., Lindroth, A., Grelle, A., Bernhofer, C., Grunwald, T., Aubinet, M., Ceulemans, R., Kowalski, A.S., Vesala, T., Rannik, U., Berbigier, P., Loustau, D., Guomundsson, J., Thorgeirsson, H., Ibrom, A., Morgenstern, K., Clement, R., Moncrieff, J., Montagnani, L., Minerbi, S., Jarvis, P.G., 2000. Respiration as the main determinant of carbon balance in European forests. Nature 404, 861–865.
van der Tol, C., Verhoef, W., Timmermans, J., Verhoef, A., Su, Z., 2009. An integrated model of soil-canopy spectral radiances, photosynthesis, fluorescence, temperature and energy balance. Biogeosciences 6, 3109–3129.
van der Tol, C., Berry, J.A., Campbell, P.K.E., Rascher, U., 2014. Models of fluorescence and photosynthesis for interpreting measurements of solar-induced chlorophyll fluorescence. J. Geophys. Res. Biogeosci. 119, 2312–2327.
Vilfan, N., Van der Tol, C., Yang, P., Wyber, R., Malenovský, Z., Robinson, S.A., Verhoef, W., 2018. Extending fluspect to simulate xanthophyll driven leaf reflectance dynamics. Remote Sens. Environ. 211, 345–356.
Vitousek, P.M., Ehrlich, P.R., Ehrlich, A.H., Matson, P.A., 1986. Human appropriation of the products of photosynthesis. Bioscience 36, 368–373.
Waldrop, M.M., 2016. The chips are down for Moore's law. Nature 530, 144–147.
Walker, A.P., Beckerman, A.P., Gu, L., Kattge, J., Cernusak, L.A., Domingues, T.F., Scales, J.C., Wohlfahrt, G., Wullschleger, S.D., Woodward, F.I., 2014. The relationship of leaf photosynthetic traits – Vcmax and Jmax – to leaf nitrogen, leaf phosphorus, and specific leaf area: a meta-analysis and modeling study. Ecol. Evol. 4, 3218–3235.
Walker, A.P., Quaife, T., van Bodegom, P.M., De Kauwe, M.G., Keenan, T.F., Joiner, J., Lomas, M.R., MacBean, N., Xu, C., Yang, X., Woodward, F.I., 2017. The impact of alternative trait-scaling hypotheses for the maximum photosynthetic carboxylation rate (Vcmax) on global gross primary production. New Phytol. 215, 1370–1386.
Wang, D., 2017. MODIS/Terra + Aqua Surface Radiation Daily/3-Hour L3 Global 5 km SIN Grid V006. NASA EOSDIS Land Processes DAAChttps://doi.org/10.5067/MODIS/MCD18A1.006.
Wang, Y.P., Jarvis, P.G., 1990. Description and validation of an array model - MAESTRO. Agric. For. Meteorol. 51, 257–280.
Wang, Y.P., Baldocchi, D., Leuning, R., Falge, E., Vesala, T., 2007. Estimating parameters in a land-surface model by applying nonlinear inversion to eddy covariance flux measurements from eight FLUXNET sites. Glob. Chang. Biol. 13, 652–670.
Wang, H., Prentice, I.C., Keenan, T.F., Davis, T.W., Wright, I.J., Cornwell, W.K., Evans, B.J., Peng, C., 2017. Towards a universal model for carbon dioxide uptake by plants. Nat. Plants 3, 734–741.
Wang, Z., Skidmore, A.K., Darvishzadeh, R., Wang, T., 2018. Mapping forest canopy nitrogen content by inversion of coupled leaf-canopy radiative transfer models from

airborne hyperspectral imagery. Agric. For. Meteorol. 253-254, 247–260.
Warnant, P., François, L., Strivay, D., Gérard, J.C., 1994. CARAIB: a global model of terrestrial biological productivity. Glob. Biogeochem. Cycles 8, 255–270.
Wei, S., Fang, H., 2016. Estimation of canopy clumping index from MISR and MODIS sensors using the normalized difference hotspot and darkspot (NDHD) method: the influence of BRDF models and solar zenith angle. Remote Sens. Environ. 187, 476–491.
Wei, Y., Liu, S., Huntzinger, D.N., Michalak, A.M., Viovy, N., Post, W.M., Schwalm, C.R., Schaefer, K., Jacobson, A.R., Lu, C., Tian, H., Ricciuto, D.M., Cook, R.B., Mao, J., Shi, X., 2014. The north American carbon program multi-scale synthesis and terrestrial model intercomparison project – part 2: environmental driver data. Geosci. Model Dev. 7, 2875–2893.
Whitley, R., Beringer, J., Hutley, L.B., Abramowitz, G., De Kauwe, M.G., Evans, B., Haverd, V., Li, L., Moore, C., Ryu, Y., Scheiter, S., Schymanski, S.J., Smith, B., Wang, Y.P., Williams, M., Yu, Q., 2017. Challenges and opportunities in land surface modelling of savanna ecosystems. Biogeosciences 14, 4711–4732.
Wiegand, C.L., Richardson, A.J., Kanemasu, E.T., 1979. Leaf area index estimates for wheat from LANDSAT and their implications for evapotranspiration and crop modeling1. Agron. J. 71, 336–342.
Wieneke, S., Burkart, A., Cendrero-Mateo, M.P., Julitta, T., Rossini, M., Schickling, A., Schmidt, M., Rascher, U., 2018. Linking photosynthesis and sun-induced fluorescence at sub-daily to seasonal scales. Remote Sens. Environ. 219, 247–258.
Williams, M., Richardson, A.D., Reichstein, M., Stoy, P.C., Peylin, P., Verbeeck, H., Carvalhais, N., Jung, M., Hollinger, D.Y., Kattge, J., Leuning, R., Luo, Y., Tomelleri, E., Trudinger, C.M., Wang, Y.P., 2009. Improving land surface models with FLUXNET data. Biogeosciences 6, 1341–1359.
Wilson, K.B., Baldocchi, D.D., Hanson, P.J., 2000. Spatial and seasonal variability of photosynthetic parameters and their relationship to leaf nitrogen in a deciduous forest. Tree Physiol. 20, 565–578.
Wofsy, S.C., Goulden, M.L., Munger, J.W., Fan, S.-M., Bakwin, P.S., Daube, B.C., Bassow, S.L., Bazzaz, F.A., 1993. Net exchange of CO_2 in a mid-latitude forest. Science 260, 1314–1317.
Wohlfahrt, G., Gerdel, K., Migliavacca, M., Rotenberg, E., Tatarinov, F., Müller, J., Hammerle, A., Julitta, T., Spielmann, F.M., Yakir, D., 2018. Sun-induced fluorescence and gross primary productivity during a heat wave. Sci. Rep. 8, 14169.
Wolf, J., West, T.O., Le Page, Y., Kyle, G.P., Zhang, X., Collatz, G.J., Imhoff, M.L., 2015. Biogenic carbon fluxes from global agricultural production and consumption. Glob. Biogeochem. Cycles 29, 1617–1639.
Woodward, F.I., Smith, T.M., Emanuel, W.R., 1995. A global land primary productivity and phytogeography model. Glob. Biogeochem. Cycles 9, 471–490.
Woodwell, G.M., Whittaker, R.H., Reiners, W.A., Likens, G.E., Delwiche, C.C., Botkin, D.B., 1978. The biota and the world carbon budget. Science 199, 141–146.
Woodwell, G.M., Hobbie, J.E., Houghton, R.A., Melillo, J.M., Moore, B., Peterson, B.J., Shaver, G.R., 1983. Global deforestation: contribution to atmospheric carbon dioxide. Science 222, 1081–1086.
Wu, J., Serbin, S.P., Xu, X., Albert, L.P., Chen, M., Meng, R., Saleska, S.R., Rogers, A., 2017. The phenology of leaf quality and its within-canopy variation is essential for accurate modeling of photosynthesis in tropical evergreen forests. Glob. Chang. Biol. 23, 4814–4827.
Xiao, X., Boles, S., Frolking, S., Salas, W., Moore, B., Li, C., He, L., Zhao, R., 2002. Observation of flooding and rice transplanting of paddy rice fields at the site to landscape scales in China using VEGETATION sensor data. Int. J. Remote Sens. 23, 3009–3022.
Xiao, J., Zhuang, Q., Law, B.E., Chen, J., Baldocchi, D.D., Cook, D.R., Oren, R., Richardson, A.D., Wharton, S., Ma, S., Martin, T.A., Verma, S.B., Suyker, A.E., Scott, R.L., Monson, R.K., Litvak, M., Hollinger, D.Y., Sun, G., Davis, K.J., Bolstad, P.V., Burns, S.P., Curtis, P.S., Drake, B.G., Falk, M., Fischer, M.L., Foster, D.R., Gu, L., Hadley, J.L., Katul, G.G., Matamala, R., McNulty, S., Meyers, T.P., Munger, J.W., Noormets, A., Oechel, W.C., Paw, U., K., T., Schmid, H.P., Starr, G., Torn, M.S., Wofsy, S.C., 2010. A continuous measure of gross primary production for the conterminous United States derived from MODIS and AmeriFlux data. Remote Sens. Environ. 114, 576–591.
Xu, L., Baldocchi, D.D., 2004. Seasonal variation in carbon dioxide exchange over a Mediterranean annual grassland in California. Agric. For. Meteorol. 123, 79–96.
Yang, P., van der Tol, C., 2018. Linking canopy scattering of far-red sun-induced chlorophyll fluorescence with reflectance. Remote Sens. Environ. 209, 456–467.
Yang, F., Ichii, K., White, M.A., Hashimoto, H., Michaelis, A.R., Votava, P., Zhu, A.X., Huete, A., Running, S.W., Nemani, R.R., 2007. Developing a continental-scale measure of gross primary production by combining MODIS and AmeriFlux data through Support Vector Machine approach. Remote Sens. Environ. 110, 109–122.
Yang, X., Tang, J., Mustard, J.F., Lee, J.-E., Rossini, M., Joiner, J., Munger, J.W., Kornfeld, A., Richardson, A.D., 2015a. Solar-induced chlorophyll fluorescence that correlates with canopy photosynthesis on diurnal and seasonal scales in a temperate deciduous forest. Geophys. Res. Lett. 42, 2977–2987.
Yang, Y., Donohue, R.J., McVicar, T.R., Roderick, M.L., 2015b. An analytical model for relating global terrestrial carbon assimilation with climate and surface conditions using a rate limitation framework. Geophys. Res. Lett. 42, 9825–9835.
Yang, B., Knyazikhin, Y., Mõttus, M., Rautiainen, M., Stenberg, P., Yan, L., Chen, C., Yan, K., Choi, S., Park, T., Myneni, R.B., 2017. Estimation of leaf area index and its sunlit portion from DSCOVR EPIC data: theoretical basis. Remote Sens. Environ. 198, 69–84.
Yang, J., Tian, H., Pan, S., Chen, G., Zhang, B., Dangal, S., 2018a. Amazon drought and forest response: largely reduced forest photosynthesis but slightly increased canopy greenness during the extreme drought of 2015/2016. Glob. Chang. Biol. 24, 1919–1934.
Yang, K., Ryu, Y., Dechant, B., Berry, J.A., Hwang, Y., Jiang, C., Kang, M., Kim, J., Kimm, H., Kornfeld, A., Yang, X., 2018b. Sun-induced chlorophyll fluorescence is more strongly related to absorbed light than to photosynthesis at half-hourly resolution in a rice paddy. Remote Sens. Environ. 216, 658–673.
Yuan, W.P., Liu, S.G., Yu, G.R., Bonnefond, J.M., Chen, J.Q., Davis, K., Desai, A.R., Goldstein, A.H., Gianelle, D., Rossi, F., Suyker, A.E., Verma, S.B., 2010. Global estimates of evapotranspiration and gross primary production based on MODIS and global meteorology data. Remote Sens. Environ. 114, 1416–1431.
Zhang, Q., Ju, W., Chen, J., Wang, H., Yang, F., Fan, W., Huang, Q., Zheng, T., Feng, Y., Zhou, Y., He, M., Qiu, F., Wang, X., Wang, J., Zhang, F., Chou, S., 2015a. Ability of the photochemical reflectance index to track light use efficiency for a sub-tropical planted coniferous forest. Remote Sens. 7, 15860.
Zhang, X., Liang, S., Wild, M., Jiang, B., 2015b. Analysis of surface incident shortwave radiation from four satellite products. Remote Sens. Environ. 165, 186–202.
Zhang, Y., Song, C., Band, L.E., Sun, G., Li, J., 2017a. Reanalysis of global terrestrial vegetation trends from MODIS products: browning or greening? Remote Sens. Environ. 191, 145–155.
Zhang, Y., Xiao, X., Wu, X., Zhou, S., Zhang, G., Qin, Y., Dong, J., 2017b. A global moderate resolution dataset of gross primary production of vegetation for 2000–2016. Earth Syst. Sci. Data 4, 170165.
Zhang, Y., Joiner, J., Gentine, P., Zhou, S., 2018a. Reduced solar-induced chlorophyll fluorescence from GOME-2 during Amazon drought caused by dataset artifacts. Glob. Chang. Biol. 24, 2229–2230.
Zhang, Z., Zhang, Y., Joiner, J., Migliavacca, M., 2018b. Angle matters: bidirectional effects impact the slope of relationship between gross primary productivity and sun-induced chlorophyll fluorescence from Orbiting Carbon Observatory-2 across biomes. Glob. Chang. Biol. 24, 5017–5020.
Zhao, M., Running, S.W., 2010. Drought-induced reduction in global terrestrial net primary production from 2000 through 2009. Science 329, 940–943.
Zhao, M.S., Heinsch, F.A., Nemani, R.R., Running, S.W., 2005. Improvements of the MODIS terrestrial gross and net primary production global data set. Remote Sens. Environ. 95, 164–176.
Zhao, M., Running, S.W., Nemani, R.R., 2006. Sensitivity of Moderate Resolution Imaging Spectroradiometer (MODIS) terrestrial primary production to the accuracy of meteorological reanalyses. J. Geophys. Res. Biogeosci. 111. https://doi.org/10.1029/2004JG000004.
Zoogman, P., Liu, X., Suleiman, R.M., Pennington, W.F., Flittner, D.E., Al-Saadi, J.A., Hilton, B.B., Nicks, D.K., Newchurch, M.J., Carr, J.L., Janz, S.J., Andraschko, M.R., Arola, A., Baker, B.D., Canova, B.P., Chan Miller, C., Cohen, R.C., Davis, J.E., Dussault, M.E., Edwards, D.P., Fishman, J., Ghulam, A., González Abad, G., Grutter, M., Herman, J.R., Houck, J., Jacob, D.J., Joiner, J., Kerridge, B.J., Kim, J., Krotkov, N.A., Lamsal, L., Li, C., Lindfors, A., Martin, R.V., McElroy, C.T., McLinden, C., Natraj, V., Neil, D.O., Nowlan, C.R., O'Sullivan, E.J., Palmer, P.I., Pierce, R.B., Pippin, M.R., Saiz-Lopez, A., Spurr, R.J.D., Szykman, J.J., Torres, O., Veefkind, J.P., Veihelmann, B., Wang, H., Wang, J., Chance, K., 2017. Tropospheric emissions: monitoring of pollution (TEMPO). J. Quant. Spectrosc. Radiat. Transf. 186, 17–39.
Zscheischler, J., Mahecha, M.D., Harmeling, S., Reichstein, M., 2013. Detection and attribution of large spatiotemporal extreme events in Earth observation data. Eco. Inform. 15, 66–73.